SYNTHETIC PEPTIDES MODULATE EPITHELIAL JUNCTIONS

by

SHENG YI

B.S., China Pharmaceutical University, 2007

A THESIS

submitted in partial fulfillment of the requirements for the degree

MASTER OF SCIENCE

Department of Biochemistry
College of Art and Sciences

KANSAS STATE UNIVERSITY
Manhattan, Kansas

2009

Approved by:

Co-Major Professor
Dr. John Tomich

Approved by:

Co-Major Professor
Dr. Bruce Schultz

Copyright

Abstract

Peptides based on the second transmembrane segment of the glycine receptor (M2GlyR) were made to provide a potential therapeutic treatment for cystic fibrosis (CF) and a latent absorption enhancer for drug delivery. For similarity of presentation, unique synthetic peptide sequences have been given alpha-numeric designations. Results are presented from studies focusing on four peptides.

In the first study, the contributions of synthetic peptides p1171, p1172 and p1173 to net transepithelial ion transport were measured as a first step toward the goal of testing whether pore length or electrostatics of pore lining residues will affect anion transport. Peptide p1130 exhibits many attributes that make it an ideal synthetic peptide for CF treatment, but has low permselectivity for anions. Therefore, it is used as a platform for modification. Peptide p1171 is doubly substituted with diaminopropionic acid at positions T13 and T17. Peptide p1172 and p1173 are separately one and two helical turn(s) inserted into the p1130 backbone. Apical exposure of MDCK monolayers to these peptides caused a rapid increase in short circuit current (I_{sc}), an indicator of net ion transport. The increase in I_{sc} caused by p1172 or p1173 was accompanied by increase in transepithelial electrical conductance (g_{te}). The electrophysiological results suggested that these modified peptides can assemble in the apical membrane of epithelial cells to form functional ion-conducting pores.

Peptide NC-1059, which provides for ion transport across epithelial cells derived from many sources, was studied further to assess cellular changes that account for increased g_{te}. NC-1059 increased I_{sc}, g_{te} and enhanced permeation of dextrans in a concentration dependent manner. Results from previous and current studies show that NC-1059 modulated the epithelial paracellular pathway by altering the distribution and abundance of junctional proteins. Immunoblotting and immunolabeling with confocal microscopy showed that NC-1059 induces reorganization of actin and causes a reduction in F-actin abundance in epithelial cells. The distributions were changed and cellular abundances were reduced of tight junction proteins occludin and ZO-1 and adherens junction proteins E-cadherin and β-catenin by NC-1059. These effects were largely reversed in 24 hr and fully recovered in 48 hr. Therefore, NC-1059 has the therapeutic potential to increase the efficiency of drug delivery across barrier membranes.

Table of Contents

List of Figures

List of Tables

Acknowledgements

I must express my sincerest thanks to the following people:

Dr. Bruce Schultz, my advisor, guided me both in academic fields and in experimental fields. He trained me of independent study and thinking, which will benefit me for my whole life.

Dr. John Tomich, my mentor, provided me with the knowledge of peptide synthesizing and purifying, which not only allowed me to master the experimental techniques but what's more important, gave me a better understanding and a wider view of my work.

Dr. Anna Zolkiewska, my committee member, is always nice and patient to answer every question of mine.

Dr. Suma Somasekharan, the one who worked on peptide NC-1059 before me, gave me many valuable suggestions and helped me a lot to follow her previous work.

I thank my laboratory members Florence Wang, Dr. Fernando Alves, Dr. Vladimir Akoyev, Pradeep Malreddy, Qian Wang for their assistances. Thanks Dr. John Tomich's laboratory members for making synthetic peptides.

Thanks to my mother, father and my pet Yangyang and the rest of my family at home. Though you are thousands of miles away from me, I love you all from the deep of my heart.

Overview

This thesis is focused on synthetic peptides that, when exposed to the apical aspect of selected epithelial cell monolayers, support anion secretion and, in some cases, modify the barrier integrity of the epithelial monolayers.

The second transmembrane segment (M2) of the spinal cord glycine receptor (GlyR), M2GlyR, is a 23-residue helical peptide (P-A-R-V-G-L-G-I-T-T-V-L-T-M-T-T-Q-S-S-G-S-R-A) that can form anion-selective channels (Reddy et al., 1993). The M2GlyR sequence was modified to generate peptides with enhanced aqueous solubility, decreased solution aggregation and improved chemical synthesis yields. Results from experiments employing four peptides that represent targeted modifications to the M2GlyR sequence are presented in Chapters 2 and 3 of this thesis.

Peptide p1130 (K-K-K-K-P-A-R-V-G-L-G-I-T-T-V-L-T-M-R-T-Q-W) was expected to be a key sequence in the development of an alternate anion pathway(s) for the treatment of cystic fibrosis. However p1130 exhibits no anion-to-cation selectivity. Therefore, peptides with modifications in hydrogen bonding potentials of pore-lining residues, electrostatics of pore-lining residues, pore length and pore rigidity were synthesized to determine underlying rules that establish anion selectivity. Results from experiments designed to test the ion channel forming ability of 3 derivatives of p1130, peptide p1171, p1172 and p1173, are presented in Chapter 2.

NC-1059 (K-K-K-K-A-A-R-V-G-L-G-I-T-T-V-L-V-T-T-I-G-L-G-V-R-A-A) is a channel-forming peptide that reversibly increases epithelial paracellular permeability (Broughman et al., 2004; Somasekharan et al., 2008; Martin et al., 2009). Cell-cell junctions link adjacent cells and regulate the movement of solutes through the paracellular route. Thus, the enhanced paracellular permeability caused by exposure to NC-1059 might reflect changes in cell junctions. Results from experiments designed to determine the abundance and distribution of key junctional proteins following NC-1059 exposure are presented in Chapter 3.

Chapter 1 provides necessary background to appreciate the lines of investigation described in Chapters 2 and 3. Tight junctions and adherens junctions are introduced along with actin cytoskeleton to provide basic concepts of cell-cell interactions. Epithelial paracellular flux and how it might be modulated are also introduced. The development of synthesized channel forming peptides is reviewed.

CHAPTER 1 - INTRODUCTION

CELL JUNCTIONS

Multicellular organisms have structures called junctions that link adjacent cells together to form tissues and organs. The three general types of cell junctions are tight junctions, adhesive junctions and gap junctions. Adhesive junctions consist of adherens junctions and desmosomes at the cell-cell interface and hemidesmosomes at the cell-matrix interface. In epithelial cells, tight junctions, adherens junctions and desmosomes form the apical junctional complex in the intercellular space between adjacent cells (Fig 1.1). Among the junctional complex, tight junctions and adherens junctions play an important role in cell adhesion and likely contribute substantially to the physiological barrier separating body compartments. The architectures and components that constitute tight junctions and adherens junctions are discussed in detail in the following sections.

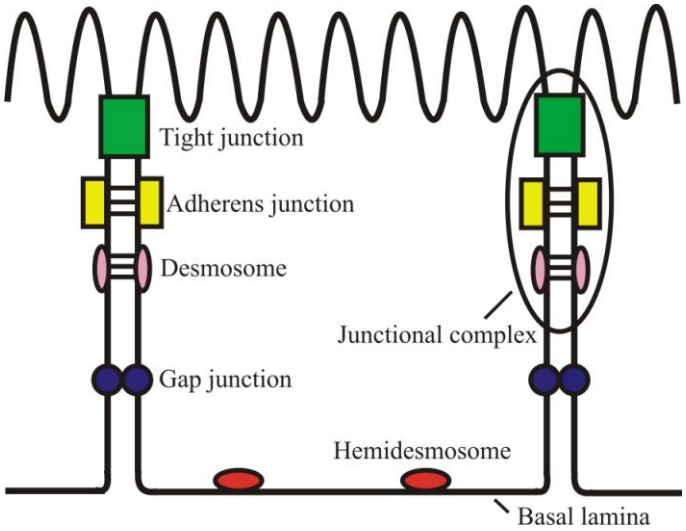

Figure 1.1 Major types of cell junctions in epithelial cells

Adhesive junctions (adherens junctions, desmosomes and hemidesmosomes) are located both at the cell-cell interface and at the cell-basal lamina interface, which allows cells to function as a unit. Tight junctions circumscribe the apical region of epithelial cells and seal the intercellular space. Gap junctions are located at the basolateral region providing direct chemical and electrical communications between adjacent cells. The junctional complex is indicated with a circle.

Tight Junctions

Tight junctions are present near the apical surface of adjacent epithelial cells and are known to perform two major functions: to act as a barrier and to act as a fence. "Barrier function" means that tight junctions act as a gatekeeper to regulate the fluid and solute movement through the paracellular space between adjacent body compartments. "Fence function" means that tight junctions block the lateral diffusive movement of lipids and integral membrane proteins in the epithelial cell membrane between the apical and basolateral surfaces of the cell, generating and maintaining a distinct region between adjacent epithelial cells.

Structure of Tight Junctions

Electron micrographs reveal the distance between adjacent epithelial cells in the non-junction region is typically 25-35 nm. The electron micrograph in Fig 1.2A shows that, at the position of tight junction proteins, the spaces between adjacent cells are quite narrow, being only ~11 nm wide, while the intercellular space is 15-20 nm in adherens junctions and desmosomes (Tsukita, Furuse & Itoh, 2001). This architecture suggests that the tight junction belt serves as a gatekeeper for paracellular permeation. Tight junctions appear as a series of regularly spaced cell-cell contact points when viewed as a high resolution transmission electron micrograph (Fig 1.2B). These contact points are called "kissing points" where the intercellular space is reduced to nearly zero. Freeze fracture replicas of tight junctions show "kisses" as well. Tight junctions intertwine to be a continuous, anastomosing network of strands that form irregular interstrand compartments on the inner leaflet of the plasma membrane and the complementary vacant grooves on the outer leaflet (Fig 1.2C).

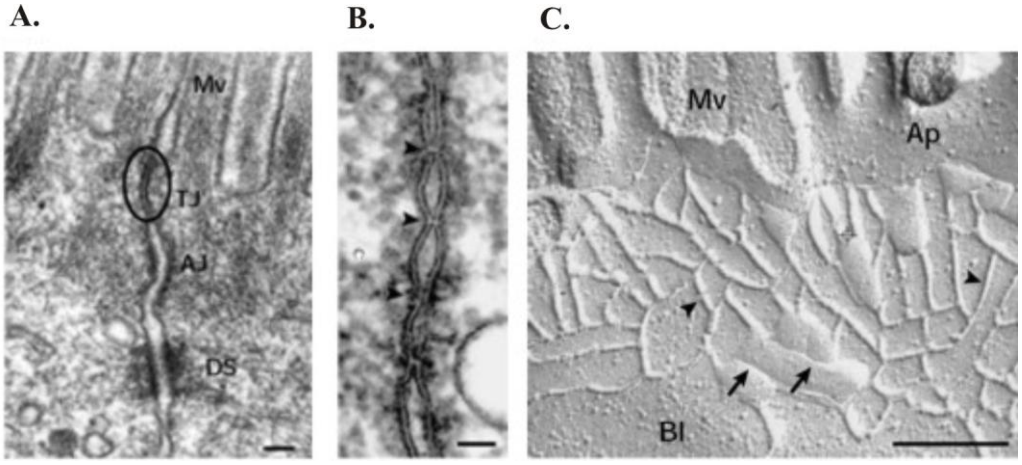

Figure 1.2 Electron micrograph representations of tight junctions

A) Transmission electron micrograph of the junctional complex in mouse intestinal epithelial cells. (Mv, microvilli; TJ, tight junction (circled); AJ, adherens junction; DS, desmosome.) Scale bar, 200 nm.
B) Ultrathin section view of tight junctions showing kissing points (arrowheads). Scale bar, 50 nm.
C) Scanning electron micrograph of freeze-fracture replica of intestinal epithelial cells representing tight junctions on the plasma membrane (arrowheads) and on the outer leaflet (arrows). (Mv, microvilli; Ap, apical membrane; Bl, basolateral membrane). Scale bar, 200 nm.
Figure as presented by (Tsukita et al., 2001).

Transmembrane Proteins of the Tight Junction

Tight junctions are "multimolecular complexes" containing three major transmembrane proteins: occludin, claudin(s) and junctional adhesion molecule(s) that are described in detail in this section. Tight junction-associated proteins containing PSD-95/DlgA/ZO-1 homology domains (PDZ domains; e.g., ZO-1, ZO-2 and ZO-3), which are described in detail in a following section, bind to occludin and claudins and link them to the actin cytoskeleton (Fig 1.3).

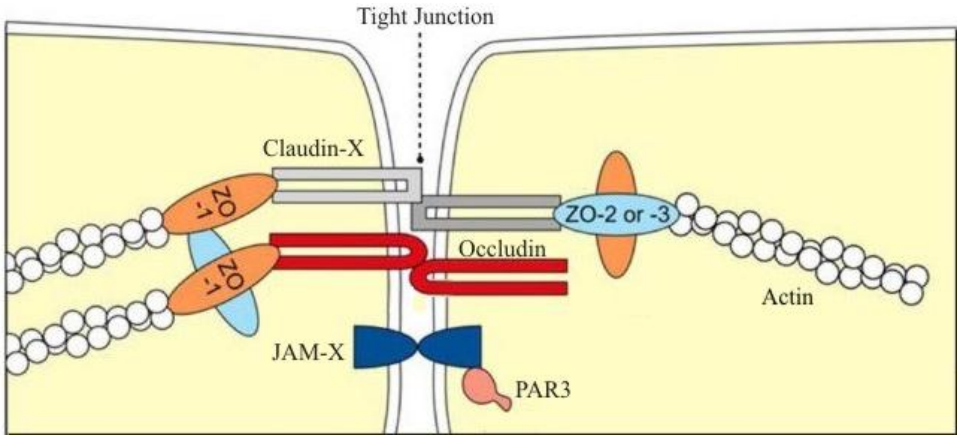

Figure 1.3 Schematic representation of the basic structural transmembrane components of tight junctions

Occludin, claudin-X and junctional adhesion molecule-X (JAM-X) are three major types of protein components of tight junctions (claudin-X indicates claudin family members 1-24, JAM-X indicates JAM family members 1-4). Proteins of the ZO family cluster claudins and occludin to form strands and link them to the actin cytoskeleton. PAR3 regulates cellular polarity.
Figure modified from (Forster et al., 2008).

Occludin

Occludin was identified as the first integral membrane protein localized at tight junctions in chick liver (Furuse et al., 1993) and was later shown to be present in T84 cells (Ando-

Akatsuka et al., 1996), a cell line derived from human colon (Dharmsathaphorn et al., 1984). Occludin has 2 isoforms arising from alternative splicing of one transcript with an identical tissue distribution (Muresan, Paul & Goodenough, 2000). Occludin is a ~65 kDa tetraspan membrane protein that has two extracellular loops (~47 residues) separated by a short cytosolic loop, along with a short amino-terminal cytosolic domain and a long carboxyl-terminal cytosolic domain (Fig 1.4). Both extracellular loops are required for cell-cell adhesion and to constitute the epithelial barrier while the carboxyl-terminal domain is required for interaction with ZO-1 and targeting at tight junctions (Mitic & Anderson, 1998).

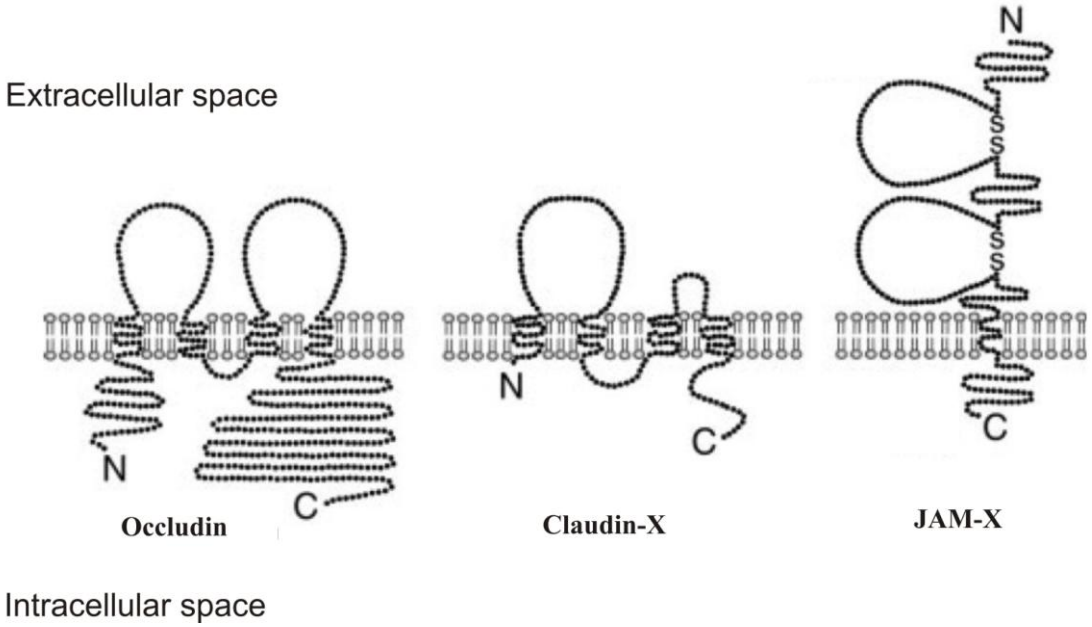

Figure 1.4 Membrane topology of tight junction proteins

Occludin is a tetraspan protein with two extracellular loops, a short cytosolic loop and a long carboxyl-terminal cytosolic domain. Claudin-X also has four transmembrane domains but has a shorter cytoplasmic tail than occludin. JAM-X has two folded IgG-like extracellular domains with disulfide bonds (claudin-X indicates claudin family members 1-24, JAM-X indicates JAM family members 1-4).

Figure modified from (Schneeberger & Lynch, 2004).

Anti-occludin antibodies labeled tight junction strands indicated that occludin directly integrates into tight junction strands (Saitou et al., 1997). However, the physiological function(s) of occludin at tight junctions is not clearly understood. Transepithelial electrical resistance (R_{te}) and paracellular permeability are parameters to study the barrier function of tight junctions. Epithelia with higher R_{te} and lower paracellular permeability have tight junctions that prevent

movement through the paracellular space of adjacent cells at a larger extent. Selective removal of occludin by exposure to synthetic peptide OCC2, corresponding to the second extracellular loop of chick occludin (GVDNPQAQMSSGYYYSPLLAMCSQAYGSTYLNYQYIYHYCTVDPQE), in culture medium decreased R_{te} and increased paracellular permeability suggesting that occludin is involved in the barrier function of tight junctions (Wong & Gumbiner, 1997). Overexpression of occludin increased R_{te} in MDCK cells but paradoxically increased paracellular flux of 4 kD FITC-dextran (Balda et al., 1991; McCarthy et al., 1996). Furthermore, occludin-deficient embryonic stem cells generated polarized epithelial cells with no observable differences in tight junction strands when compared to wild-type epithelial cells as shown by immunofluorescence microscopy and transmission electron microscopy (Saitou et al., 1998). Occludin-deficient mice exhibited no global epithelial defect. Rather, the phenotype was characterized by postnatal growth retardation, chronic inflammation and hyperplasia of the gastric epithelium, calcification in the brain and abnormalities in the testis, salivary gland and bone (Saitou et al., 2000). Therefore, although the fundamental role of occludin is not yet defined, occludin is involved in tight junction strands and contributes to barrier function of tight junctions.

Claudins

Claudins constitute a multigene family of at least 24 isoforms in mammals with molecular masses ranging from 20 kDa to 27 kDa. Like occludin, claudins are four transmembrane domain proteins, although they exhibit no sequence similarity to occludin. Claudins have a large (~52 residues) extracellular loop and a small (~25 residues) extracellular loop separated by an intercellular loop along with a very short amino-terminal cytoplasmic sequence (~7 residues) and a carboxyl-terminal cytoplasmic sequence (Fig 1.4). The C-terminal ends differ in length between isoforms (21-63 residues), but all except claudin-12 end in YV, a sequence that binds to the PDZ domains of tight junction-associated proteins such as MAGUKs, ZO-1, ZO-2, ZO-3 (Itoh et al., 1999), MUPP1 (Hamazaki et al., 2002; Roh et al., 2002) and PATJ (Roh et al., 2002). Inducible expression of claudin-1 that lacks its C-terminal YV residues formed aberrant tight junction strands with no associated ZO-1, which suggests that the C-terminus plays a fundamental role in the interaction between claudins and tight junction-associated proteins (McCarthy et al., 2000).

Claudin isoform expression is organ and tissue specific (Table 1.1). Moreover, two or more distinct claudins are coexpressed in most cell types in various combinations and distinct claudins are coincorporated into individual tight junction strands (Furuse, Sasaki & Tsukita, 1999). The R_{te} difference between MDCK I and MDCK II cells might be due to the expression of different claudin isoforms. MDCK I cells express primarily claudin-1 and claudin-4 whereas MDCK II cells, which express claudin-2 as well as claudin-1 and claudin-4, have a 30–60 fold lower R_{te}. Transfecting claudin-2 into MDCK I cells resulted in reduced R_{te} values (Tsukita et al., 2001).

Table 1.1 Claudin gene families

Claudins*	Expression#						
	Heart	Brain	Lung	Liver	Kidney	Testis	Other
Claudin-1	+	+	+	+	+	+	
Claudin-2	-	-	-	+	+	-	
Claudin-3	-	-	+	+	+	±	
Claudin-4	-	-	+	-	+	-	
Claudin-5	+	+	+	+	+	+	Endothelial cells
Claudin-6	-	-	-	-	-	-	Embryonic tissues
Claudin-7	-	-	+	-	+	±	
Claudin-8	-	-	+	±	+	±	
Claudin-10	ND	ND	ND	ND	ND	ND	
Claudin-11	-	+	-	-	-	+	Oligodendrocytes, Sertoli cells
Claudin-14	-	-	-	+	+	ND	Hair cells in the Corti organ
Claudin-16	-	-	-	-	+	ND	Thick ascending limb of Henle

* Claudin-9,-12,-13, -15 and 17-24 have not been characterized well.

Detected by northern blotting.

+, detectable expression; -, expression not detected; ±, expression variably detectable.

ND, not determined.

Table as presented by (Tsukita et al., 2001).

Claudins play important roles in the formation of tight junction fibers and in regulating paracellular selectivity to ions. Immuno-replica electron microscopy revealed that claudins constitute the backbone of tight-junction strands. Tight junction strands can be reconstituted by introducing a single gene encoding claudin-1 or -2 into mouse L-cells, a fibroblastic cell line, that otherwise lacks tight junctions (Furuse et al., 1998). Overexpression or knockdown of

selected claudins in epithelial cell lines shows that claudin-1, -4, -5, -8, -11 or -14 expression increases R_{te} by decreasing cation permeability while claudin-2, -10b or -15 expression decreases R_{te} by acting as cation-selective pores (Angelow, Ahlstrom & Yu, 2008).

Claudins also effects paracellular charge selectivity. Paracellular pathway, discussed in details in the following section, is the route between cells. Solutes travel through junctional proteins in the paracellular pathway to pass across epithelial layers. The first extracellular domain of claudin-15 has 3 acidic residues. When those acidic amino acids are replaced with basic residues, the dilution potential on MDCK monolayers dropped from 7.6 ± 0.6 to -7.1 ± 0.7 mV, indicating that the ratio of P_{Na} to P_{Cl} decreased after the mutation of claudin-15 (Colegio et al., 2002). It suggested that claudin-15 is important in cation-selective permeation. Claudin-4 has a positively charged residue in the first extracellular domain. When claudin-4 is expressed in MDCK monolayers, dilution potential decreased from 8.4 ± 0.4 to 4.2 ± 0.9 mV, which suggested that Na^+ permeability decreased. When this positively charged residue is mutated to a negatively charged residue, Na^+ permeability increased (Colegio et al., 2002). Experiments had shown that not only claudin-4, but also claudin-10a (Van Itallie & Anderson, 2006) and possibly claudin-7 (Hou et al., 2006) may provide for anion-selective permeation. Therefore, claudins create charge-selective channels in the paracellular space (Van Itallie & Anderson, 2004).

Claudins not only form charge and ion selective pores, but also influence the formation of size-selective paracellular pores that control the movement of noncharged solutes. Overexpression of claudin-2 increased the apparent permeability (P_{app}) for polyethylene glycols (PEGs) that can traverse a pore (< 4 Å) but did not change the permeability for larger PEGs. That is, expression of claudin-2 increases the number of small pores. However, the overexpression of claudin-4, -14 and -18 had no effect on pore number or pore size but significantly increased R_{te} (Van Itallie et al., 2008).

Junction-associated adhesion molecules (JAMs)

Junctional adhesion molecules (JAMs; ~40 kDa) are members of the immunoglobulin (Ig) superfamily that localize to the tight junctions of both epithelial and endothelial cells. JAMs have a single transmembrane domain, two folded immunoglobulin-like domains in the extracellular space with intrachain disulfide bonds and a carboxyl-terminal cytoplasmic sequence

that ends with a PDZ-binding motif, which enables it to interact with structural and signaling proteins (Fig 1.4). JAMs have at least 4 isoforms, among which JAM-1 is best described.

Both confocal and immunoelectron microscopy data showed that JAMs are concentrated at the apical region of intercellular junctions (Malergue et al., 1998). CHO cells (Malergue et al., 1998) and L cells (Itoh et al., 2001) expressing JAM did not form tight junction-like strands, but formed planar aggregates through their lateral self-association. JAM-1 forms homophilic adhesion between adjacent cells and directly associates with ZO-1, PAR-3 (Itoh et al., 2001), occludin and cingulin (Bazzoni et al., 2000). Thus, JAM is involved in cell-cell adhesion assembly of epithelial cells (Forster et al., 2008).

Tight junction-associated proteins

Peripheral membrane proteins that have PDZ domains, such as ZO-1, ZO-2 and ZO-3, play curial roles in the formation of tight junctions or in the intracellular signaling originating from tight junctions (Adachi et al., 2006). PDZ domains are protein-protein interaction domains first described in the proteins PSD-95, DLG and ZO-1 (Tsukita et al., 2001). ZO-1 (zonula occludens-1, ~220 kDa), ZO-2 (~160 kDa) and ZO-3 (~130 kDa) have sequences that are similar to one another and all of them have three PDZ domains, one src homology region 3 (SH3) domain and one guanylate kinase-like (GUK) domain in their NH_2 termini, for which reason they are called MAGUKs (for membrane-associated guanylate kinase proteins; Fig 1.5) (Adachi et al., 2006; Furuse et al., 1994; Kniesel & Wolburg, 2000).

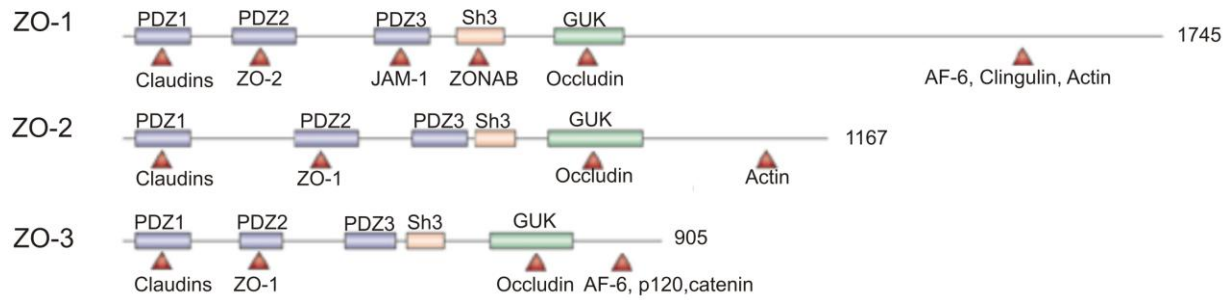

Figure 1.5 Schematic representation of ZO-1, ZO-2 and ZO-3

The PDZ domains responsible for intermolecular association are indicated by arrowheads. (ZONAB, ZO-1-associated nucleic acid binding protein; AF-6, ALL-1 fusion partner from chromosome 6; GUK, guanylate-kinase-like domain; SH3, src homology region 3; SAF-B, scaffold attachment factor-B).

Figure modified from (Schneeberger & Lynch, 2004).

ZO-1 was the first identified tight junction-associated protein and remains the best described (Stevenson et al., 1986). ZO-1 links to claudins through its PDZ1 domain, to ZO-2, ZO-3 and a gap junction protein, connexin 43, through its PDZ-2 domain, to JAM-1 through its PDZ-3 domain, to ZO-1 nucleic acid binding protein (ZONAB) through its SH3 domain, to occludin through its GUK domain, to Ras target AF-6 (Yamamoto et al., 1997), cingulin (Cordenonsi et al., 1999) and most important, the actin cytoskeleton through its proline-rich C terminus (Tsukita et al., 2001). A knockout of ZO-1 in mouse epithelial cells resulted in marked retardation in the formation of tight junctions when the epithelial polarization was initiated by switching from low Ca^{2+} media to normal Ca^{2+} media (Umeda et al., 2004). This outcome suggested that no tight junctions are formed without tight junction-associated proteins. However, in non-epithelial cells lacking tight junctions such as cardiac muscle cells or in epithelial cells lacking well developed tight junctions such as hepatocytes, ZO-1 was also reported to be enriched in adherens junctions (Kniesel & Wolburg, 2000). Since PDZ-containing proteins have diverse interactions with tight junction proteins and serve as anchors to the actin cytoskeleton, they are crucial in tight junctions.

Adherens Junctions

Adherens junctions are multiprotein complexes that mediate cell-cell adhesion. In polarized epithelial cells, adherens junctions appear as zipper-like zones that circumscribe entire cells and thus are also called “the adhesion belt”. Adherens junctions consist of two basic adhesive units: the nectin-afadin adhesion complex and the cadherin-catenin ‘core’ adhesion complex, which is studied more widely (Fig 1.6). Nectins and nectin-like molecules are members of the immunoglobulin-like superfamily that participates in calcium-independent cell adhesion. Nectins undergo both trans-homophilic and trans-heterophilic interactions, interact with an actin-binding protein AF6/afadin and play roles in the formation of cell-cell junctions (Ebnet, 2008).

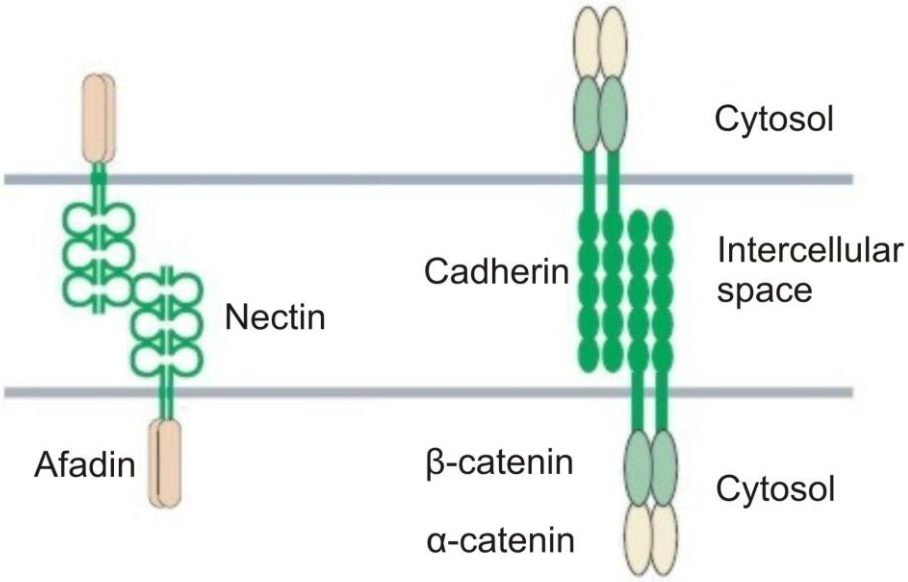

Figure 1.6 Schematic representations of the basic structural components of the adherens junctions
Shown are the cadherin-catenin complex and the nectin-afadin complex.
Figure modified from (Ogita, Ikeda & Takai, 2008).

Cadherin-catenin complex

Cadherins constitute a group of calcium-dependent adhesive glycoproteins present in the plasma membranes of most animal cells. Upon calcium binding, the extracellular domains of cadherins rigidifies to form a rod-like ectodomain that allows them to mediate cell-cell adhesion (Tai, Kim & Schuman, 2008).

More than 100 cadherin family members have been described and divided into 7 subfamilies varying in numbers of structurally similar subunits (called repeats) and in the structure of their cytosolic ends. The adherens junctions contain classical Type I and Type II cadherins. Among those cadherins in adherens junctions, E-cadherins, a "classical" Type I cadherin is best characterized. E-cadherins associate as homodimers in the plasma membranes and interact with homodimers in the neighboring cell through their extracellular domains (Resink et al., 2009). Adhesion is conferred by the interaction of the cytoplasmic carboxyl-terminal regions of E-cadherins to β-catenin, which further binds to α-catenins to link E-cadherins to actin filaments (Rudini & Dejana, 2008). β-catenin is a central player for full adhesive function due to its bridge function. Phosphorylation of β-catenin significantly reduces the affinity of cadherin for

β-catenin and results in disassembly of cadherin-containing complexes and affects cell-cell adhesion (Gloushankova, 2008; Roura et al., 1999).

Cell junctions provide important adhesive contacts between adjacent cells. Although tight junctions and adherens junctions contain different transmembrane proteins, they are both anchored to actin filaments, which are key components of the cytoskeleton. The efficient formation and maintenance of cell adhesion also requires the involvement of the actin cytoskeleton (Miyoshi & Takai, 2008). Therefore, actin filaments are discussed in the next section.

Actin Cytoskeleton

The equilibrium between G-actin and F-actin

Actin is an abundant protein with a molecular mass of ~42 kDa, which folds into a U-shape with a central cavity that binds ATP or ADP. Actin exists in two forms: a globular monomeric form (G-actin) and as a polymerized microfilament (filamentous F-actin). G-actin can polymerize reversibly into several different and distinct polymers. Actin polymerization follows a nucleation-elongation scheme that ultimately forms two parallel helical F-actin strands with roughly 13.5 actin monomers per turn. To start actin filament growth, the ADP bound G-actin is nucleotide exchanged to its ATP-bound form (Fig 1.7). Those ATP-bound G-actin monomers form dimmers and then trimers, which act as "nuclei" for consequent filament growth. Nucleation of ATP-bound G-actin monomers is unfavorable since these "nucleus" are unstable. However, elongation of actin filaments is favorable and once the elongation step is started, actin filaments grow rapidly (Sept & McCammon, 2001). The growing end is called the plus (+) end while the non-growing end is called the minus (-) end. Once the actin filament is formed, the ATP bound to G-actin is hydrolyzed slowly to ADP and actin filaments depolymerize from the minus end.

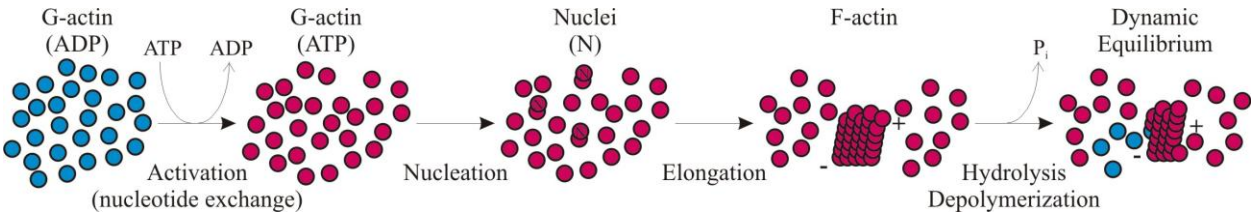

Figure 1.7 Model of microfilament dynamic equilibrium

ATP-bound G-actin monomers polymerize to form long filamentous polymers F-actin. Aged F-actin hydrolyzes to ADP-bound G-actin and depolymerize. Actin recycles the processes of polymerization and depolymerization.

G-actin and F-actin will exist in a dynamic equilibrium. Specific proteins and plasma membrane lipids can affect polymer dynamics at the ends of microfilaments to enhance or reduce the proportion of F-actin. Inositol phospholipids, the actin-related protein (Arp) 2/3 complex and the small regulatory GTP-binding proteins known as Rac, Rho, and Cdc42 are examples of cellular components that affect the G-actin to F-actin ratio. Some drugs have similar effects on actin. Cytochalasins, a group of fungal metabolites, bind to the plus ends of actin filament and prevent addition of G-actin subunits to existing polymerized microfilaments. As G-actin subunits are lost from the minus ends, actin filaments disappear (Cooper, 1987). Latrunculin A, another actin depolymerization reagent, binds to actin monomers and prevents their addition to the plus end of microfilaments (Ayscough, 2005). In contrast, Phalloidin functions as an actin stabilizing reagent by binding to actin filaments, preventing depolymerization and finally shifting the equilibrium between filaments and monomers toward F-actin (Cooper, 1987).

Functions of Actin Microfilaments

Actin microfilaments play multiple roles in promoting cell movement, developing and maintaining cell shape, establishing intercellular adhesion and supporting signal transduction. The extracellular seal produced by tight junctions and adherens junctions is dependent on actin microfilaments (Miyoshi & Takai, 2008). Adding the actin-disrupting drug cytochalsin D or latrunculin A to epithelial cells resulted in a significant decrease in R_{te} (Stevenson & Begg, 1994) as well as redistribution of tight junction proteins (Madara, Barenberg & Carlson, 1986). Meanwhile, changes in cell permeability and in tight junctions are often concomitant with changes in actin filament organization. For example, cytokines such as the interleukins (ILs), tumor necrosis factor alpha (TNFα) and interferon gamma (IFNγ), not only reduce expression of tight junction proteins but also promote reorganization of the actin cytoskeleton (Forster et al., 2008). Rho protein causes a dramatic increase in tight junction permeability with concomitant actin reorganization as well (Jou, Schneeberger & Nelson, 1998; Nusrat et al., 1995).

The outcomes, that altering the actin cytoskeleton destabilizes the junctional complex and vice versa, suggested that cell junctions physically link to the actin cytoskeleton. In epithelial

cells, actin cytoskeletons, together with tight junctions and adherens junctions, divide the plasma membrane into apical and basolateral domains and, thus, contribute to epithelial cell polarity (Miyoshi & Takai, 2008). These structures are also involved when solutes cross epithelial cell monolayers through the paracellular space as discussed in detail in the next section.

Epithelial Paracellular Flux

Transcellular pathway and paracellular pathway

Transepithelial solute movement occurs through both transcellular and paracellular pathways (Fig 1.8). In the transcellular pathway, substances travel across the apical membrane, the cytoplasm and basolateral membrane in a directional, energy dependent way controlled by specific membrane transporters and channels (Anderson, 2001). In the paracellular pathway, solutes pass through tight junctions and adherens junctions in the extracellular space between adjacent cells. The paracellular pathway allows for the passive movement of material down electrochemical gradients that are externally imposed or created by transcellular mechanisms (Van Itallie & Anderson, 2006).

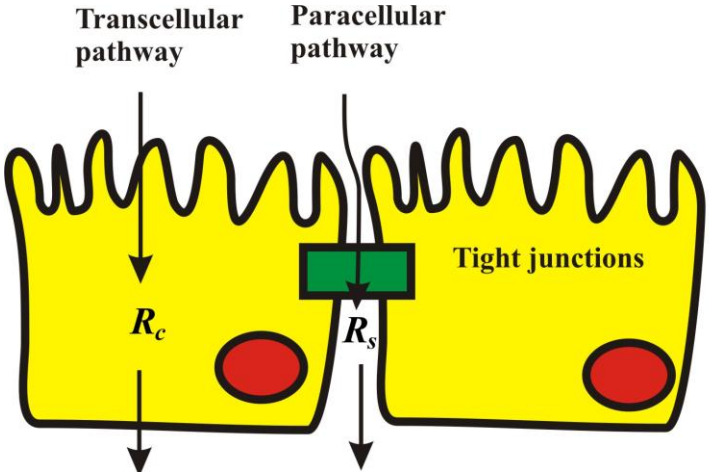

Figure 1.8 Schematic diagram of epithelial cell transport pathways

There are two pathways through which solutes cross epithelial and endothelial cellular sheets: the transcellular route and the paracellular route. $R_{s,}$ paracellular resistance; R_c, transcellular resistance; R_{te}, transepithelial resistance.

The paracellular pathway can be studied by measuring R_{te} and the permeability to labeled tracer molecules (Matter & Balda, 2003). The measured R_{te} is the parallel connection of the paracellular resistance R_s and the transcellular resistance R_c (R_{te}= (R_c × R_s) / (R_c + R_s)). In commonly studied epithelia, the paracellular resistance is much less than the transcellular resistance. For example, in small intestine, gall bladder, or cell lines such as MDCK and CaCo-2, R_{te} is ~60-250 Ω cm^2 while the R_c is on the order of 1,000-10,000 Ω cm^2 (Madara, 1989). Thus, R_{te} largely reflects the paracellular resistance and the paracellular pathway is the major site for transepithelial permeation (Blikslager et al., 2007). Since tight junctions are often rate limiting in solute movement through the paracellular pathway, alternations in R_{te} are often used as an index of tight junction permeability (Madara, 1989).

Paracellular permeability can be assessed by quantifying the movement of labeled tracer molecules. Tracer molecules of various sizes, such as mannitol, inulin and dextran labeled with radioisotopes or fluorescent tags are used. For example, dextran can only permeate the paracellular route. Therefore, permeation by selected sizes of dextran provides evidence regarding the "openness" and size exclusion for this pathway. Compared with measurement of R_{te}, tracer molecule permeability detection assay can be taken over a longer period of time but allows the quantification of slow diffusion and size selectivity of the paracellular barrier (Kapus & Szaszi, 2006).

Modulation of paracellular pathway and drug delivery

Therapeutic agents typically cross epithelial and endothelial cell layers to reach their targets. Lipophilic solutes can cross biological membranes by simple diffusion and can be selectively transported by channel, pumps and carriers present in plasma membranes (Gonzalez-Mariscal, Hernandez & Vega, 2008). For hydrophilic drugs that cannot passively cross biological membranes, the paracellular pathway can be a major route for absorption (Salama, Eddington & Fasano, 2006). Tight junctions, which exist in both epithelial and endothelial cells, strictly regulate the movement of solutes through the paracellular route. Therefore, strategies to open tight junctions were designed to modulate the bioavailability of hydrophilic drugs.

One method to enhance paracellular solute passage is to uncouple the protein-protein interactions in the intercellular space of tight junctions. Wong and Gumbiner synthesized a peptide corresponding to the second loop of chicken occluding. The synthetic peptide competed

with the interactions of occludin between adjacent cells, reducing R_{te} from ~6000 Ω cm^2 to ~900 Ω cm^2 and increasing the flux of paracellular tracers including mannitol (hydrodynamic radius ~ 4 angstrom), inulin (hydrodynamic radius ~10-14 angstrom) and dextran 3,000 by ~10 fold across A6 cell monolayers, a cell line derived from *Xenopus* kidney epithelium (Liang et al., 2000; Nusrat et al., 2005; Wong & Gumbiner, 1997). Therefore, by changing peptide corresponding to external portion of tight junction proteins, paracellular permeability can be enhanced.

Specific degradation of mRNA coding for individual tight junction proteins can also affect the paracellular movement. Yu silenced the expression of occludin using siRNA in MDCK cells. Occludin expression was reduced by 96-98% and the epithelial cells had a 50% to 75% lower maximum R_{te} compared with vehicle (Yu et al., 2005). siRNA knock down of claudin 4 resulted in a significant R_{te} decrease as well as dextran permeability increase in respiratory cells (Gonzalez-Mariscal, Nava & Hernandez, 2005). The silenced expression of tight junction proteins reduced R_{te} and increased paracellular permeability.

Another common method to open the paracellular route is the use of toxins and proteins derived from microorganisms. Bacterial toxins, such as *Clostridium difficile* enterotoxins, *Esoherichia coli* enterotoxins, *Vibrio cholerae* enterotoxin (zonula occludens toxin) are capable of rearranging the actin cytoskeleton, affecting specific tight junction proteins, and therefore increasing the paracellular permeability (Fasano, 2000; Salama et al., 2006). Among these, the role of *Clostridium difficile* is probably best known. The enterotoxin (toxin A) and the cytotoxin (toxin B) made the GTP-binding protein Rho inactive and degraded F-actin (Just et al., 1994). Therefore, purified Toxin A from *Clostridium difficile* at a concentration of as low as 7×10^{-1} μg/ml (3×10^{-9} M) decreased the R_{te} across T84 cell monolayers to 20% of its original value (Hecht et al., 1988). Thus, through a rearrangement of the actin cytoskeleton, bacterial toxins can affect paracellular pathway.

Opening the paracellular pathway by changing the molecular constituents of tight junctions can be used as an effective method for hydrophilic drug delivery. However, opening of paracellular pathway might also increase the risk of introducing organisms or toxins that are typically confined to the intestinal lumen. Therefore, identifying strategies to open the paracellular route while minimizing the risk for movement of potentially toxic luminal components is a high priority.

Synthetic Peptides

Synthesized peptides to enhance paracellular permeability

The glycine receptor (GlyR), $GABA_A$ receptor ($GABA_AR$), 5-HT_3 receptor and nicotinic acetylcholine receptor (nAChR) belong to a superfamily of ligand-gated channels formed by a pentameric arrangement of subunits having four predicted transmembrane segments, M1-M4, among which, the M2 segments line a hydrophilic ion conductive pathway. The M2 segment of the glycine receptor, M2GlyR, a 23-residue helical peptide with a sequence of P-A-R-V-G-L-G-I-T-T-V-L-T-M-T-T-Q-S-S-G-S-R-A, was synthesized by members of this laboratory as a first step in developing synthetic peptides that could form ion selective channels (Reddy et al., 1993).

To enhance the aqueous solubility of the M2GlyR sequence, lysine residues were added systematically to either the C-terminus (CK_4-M2GlyR, P-A-R-V-G-L-G-I-T-T-V-L-T-M-T-T-Q-S-S-G-S-R-A-K-K-K-K) or the N-terminus (NK_4-M2GlyR, K-K-K-K-P-A-R-V-G-L-G-I-T-T-V-L-T-M-T-T-Q-S-S-G-S-R-A) (Tomich et al., 1998). Initially the CK_4-M2GlyR sequence was tested using MDCK monolayers, a cell line derived from canine kidney (Broughman et al., 2001; Wallace et al., 1997b). When exposed to the apical membrane of MDCK cells, CK_4-M2GlyR appeared to generate chloride-selective channels in the apical membrane and to induce sustained transepithelial secretion of Cl^- and fluid. NMR and molecular modeling results showed that lysine residues in CK_4-M2GlyR form a C-terminus cap structure by folding back to form hydrogen bonds with backbone carbonyl groups and hydroxyl side chains of residues in the helical segment of the peptide, thus impairing both channel conductance and membrane insertion (Broughman et al., 2002a). Similar analysis of NK_4-M2GlyR did not reveal a capping structure but instead showed a much higher channel forming activity. Since "peptide-based channel replacement therapy" requires a channel-forming peptide with substantial aqueous solubility and little solution aggregation, a series of C- and N- terminus oligo-lysyl-modified peptides with amino acid residues deleted from the end opposite the lysine tail were synthesized and tested (Broughman et al., 2002b). The results show that a region of NK_4-M2GlyR near the C terminus promotes aqueous aggregation and that removal of 11 amino acids from the C-terminal end eliminated aggregation. The N-terminus contributes to helical bundle formation, which is necessary for channel activity, and removal of 5 amino acids from the N-terminus decreased significantly the channel-forming ability.

A palindromic sequence was designed based on the bundle-forming, non-aggregating, NH_4-terminal portion (underlined) of M2GlyR positioned around a central leucine (K-K-K-K-P-A-R-V-G-L-G-I-T-T-V-L-V-T-T-I-G-L-G-V-R-A-P). In order to improve the chemical synthesis yields, the C- and N-terminal proline residues were replaced with alanines. The resulting palindromic sequence (K-K-K-K-A-A-R-V-G-L-G-I-T-T-V-L-V-T-T-I-G-L-G-V-R-A-A), designated NC-1059, was synthesized and analyzed for solubility, aggregation and channel-forming activity (Broughman et al., 2004). NC-1059 reversibly increases I_{sc}, g_{te} and dextran permeation in a concentration dependent manner when exposed to epithelial cells (Broughman et al., 2004; Somasekharan et al., 2008).

Peptide characteristics that potentially enhance anion selectivity

One final purpose in studying variants of M2GlyR is to synthesize an ideal sequence, which exhibits aqueous solubility, little self-association in aqueous solutions, low aqueous concentration required to achieve ion channel formation in cell membranes, and high anion to cation selectivity of the resulting channels. In those M2GlyR derived peptides, p1130 (K-K-K-K-P-A-R-V-G-L-G-I-T-T-V-L-T-M-R-T-Q-W) exhibits enhanced aqueous solubility as a monomer and undergoes supramolecular assembly in the biological membranes at low aqueous concentration. However, the pores formed by p1130 show no anion selectivity. Therefore, peptides based on the p1130 amino acid sequence, with alterations in: 1) hydrogen bonding potentials of pore lining residues; 2) electrostatics of pore lining residues; 3) pore length; and 4) pore rigidity, were synthesized and tested in an attempt to determine which parameter(s) would affect anion selectivity.

Peptide p1171 (K-K-K-K-P-A-R-V-G-L-G-I-Dap-T-V-L-Dap-M-R-T-Q-W) is a peptide that contains the unusual amino acid diaminopropionic acid (L-Dap) at positions 13 and 17 in the p1130 sequence. It was synthesized to test whether changes in pore residue electrostatics by adding two positively charged amino acids would affect ion channel-forming function and anion selectivity. Peptide p1172 (K-K-K-K-P-A-R-V-G-L-G-I-L-T-G-I-T-T-V-L-T-M-R-T-Q-W) is a peptide containing one more internal helical turn than p1130 while p1173 (K-K-K-K-P-A-R-V-G-L-G-L-T-G-I-L-T-G-I-T-T-V-L-T-M-R-T-Q-W) is a peptide containing two additional internal helical turns than p1130. A structural model of peptide p1130 made by Jianhan Chen indicates an apparent thinning of membrane near the ion channel. Peptides p1172 and p1173

with longer membrane spanning lengths should induce less membrane thinning. Therefore, they were synthesized to test whether eliminating membrane thinning by increasing pore length would affect ion channel-forming function or anion selectivity.

Other sequence modifications based on p1130 are being studied to find an ideal channel-forming sequence with high anion selectivity. These studies are in progress and are outside the scope of current thesis.

Goals of Study

In this study, MECK cells were used as an experimental model to test for the channel-forming functions of novel peptides whose sequence is based on the amino acid sequence of p1130, with the final purpose of identifying compounds that can enhance apical Cl^- conductance and serve as a substitute for endogenous Cl^- channels that are defective in cystic fibrosis (Chapter 2).

Chapter 3 focuses on the effects of NC-1059 on MDCK cell monolayers. The cellular expressions and distributions of tight junction proteins, adherens junction proteins and actin cytoskeleton were tested to attain a better understanding of how NC-1059 increased epithelial paracellular permeability. Recovery of expression and distribution of junction protein and actin as well as R_{te} across MDCK monolayers after 24 and 48 hours NC-1059 treatment were also studied. The low cytotoxicity of NC-1059 indicates that NC-1059 can be used as an absorption enhancer to increase the efficiency of drug delivery across barrier membranes.

References

Adachi, M., Inoko, A., Hata, M., Furuse, K., Umeda, K., Itoh, M., Tsukita, S. 2006. Normal establishment of epithelial tight junctions in mice and cultured cells lacking expression of ZO-3, a tight-junction MAGUK protein. *Mol Cell Biol* **26:**9003-15

Anderson, J.M. 2001. Molecular structure of tight junctions and their role in epithelial transport. *News Physiol Sci* **16:**126-30

Ando-Akatsuka, Y., Saitou, M., Hirase, T., Kishi, M., Sakakibara, A., Itoh, M., Yonemura, S., Furuse, M., Tsukita, S. 1996. Interspecies diversity of the occludin sequence: cDNA cloning of human, mouse, dog, and rat-kangaroo homologues. *J Cell Biol* **133:**43-7

Angelow, S., Ahlstrom, R., Yu, A.S. 2008. Biology of claudins. *Am J Physiol Renal Physiol* **295:**F867-76

Ayscough, K.R. 2005. Coupling actin dynamics to the endocytic process in Saccharomyces cerevisiae. *Protoplasma* **226:**81-8

Balda, M.S., Whitney, J.A., Flores, C., Gonzalez, S., Cereijido, M., Matter, K. 1996. Functional dissociation of paracellular permeability and transepithelial electrical resistance and disruption of the apical-basolateral intramembrane diffusion barrier by expression of a mutant tight junction membrane protein. *J Cell Biol* **134:**1031-49

Bazzoni, G., Martinez-Estrada, O.M., Orsenigo, F., Cordenonsi, M., Citi, S., Dejana, E. 2000. Interaction of junctional adhesion molecule with the tight junction components ZO-1, cingulin, and occludin. *J Biol Chem* **275:**20520-6

Blikslager, A.T., Moeser, A.J., Gookin, J.L., Jones, S.L., Odle, J. 2007. Restoration of barrier function in injured intestinal mucosa. *Physiol Rev* **87:**545-64

Broughman, J.R., Brandt, R.M., Hastings, C., Iwamoto, T., Tomich, J.M., Schultz, B.D. 2004. Channel-forming peptide modulates transepithelial electrical conductance and solute permeability. *Am J Physiol Cell Physiol* **286:**C1312-23

Broughman, J.R., Mitchell, K.E., Sedlacek, R.L., Iwamoto, T., Tomich, J.M., Schultz, B.D. 2001. NH(2)-terminal modification of a channel-forming peptide increases capacity for epithelial anion secretion. *Am J Physiol Cell Physiol* **280:**C451-8

Broughman, J.R., Shank, L.P., Prakash, O., Schultz, B.D., Iwamoto, T., Tomich, J.M., Mitchell, K. 2002a. Structural implications of placing cationic residues at either the NH2- or COOH-terminus in a pore-forming synthetic peptide. *J Membr Biol* **190:**93-103

Broughman, J.R., Shank, L.P., Takeguchi, W., Schultz, B.D., Iwamoto, T., Mitchell, K.E., Tomich, J.M. 2002b. Distinct structural elements that direct solution aggregation and membrane assembly in the channel-forming peptide M2GlyR. *Biochemistry* **41:**7350-8

Cooper, J.A. 1987. Effects of cytochalasin and phalloidin on actin. *J Cell Biol* **105:**1473-8

Colegio, O.R., Van Itallie, C.M., McCrea, H.J., Rahner, C., Anderson, J.M. 2002. Claudins create charge-selective channels in the paracellular pathway between epithelial cells. *Am J Physiol Cell Physiol* **283:**C142-7

Cordenonsi, M., D'Atri, F., Hammar, E., Parry, D.A., Kendrick-Jones, J., Shore, D., Citi, S. 1999. Cingulin contains globular and coiled-coil domains and interacts with ZO-1, ZO-2, ZO-3, and myosin. *J Cell Biol* **147:**1569-82

Dharmsathaphorn, K., McRoberts, J.A., Mandel, K.G., Tisdale, L.D., Masui, H. 1984. A human colonic tumor cell line that maintains vectorial electrolyte transport. *Am J Physiol* **246:**G204-8

Ebnet, K. 2008. Organization of multiprotein complexes at cell-cell junctions. *Histochem Cell Biol* **130:**1-20

Fasano, A. 2000. Regulation of intercellular tight junctions by zonula occludens toxin and its eukaryotic analogue zonulin. *Ann N Y Acad Sci* **915:**214-22

Forster, C., Burek, M., Romero, I.A., Weksler, B., Couraud, P.O., Drenckhahn, D. 2008. Differential effects of hydrocortisone and TNFalpha on tight junction proteins in an in vitro model of the human blood-brain barrier. *J Physiol* **586:**1937-49

Furuse, M., Hirase, T., Itoh, M., Nagafuchi, A., Yonemura, S., Tsukita, S. 1993. Occludin: a novel integral membrane protein localizing at tight junctions. *J Cell Biol* **123:**1777-88

Furuse, M., Itoh, M., Hirase, T., Nagafuchi, A., Yonemura, S., Tsukita, S. 1994. Direct association of occludin with ZO-1 and its possible involvement in the localization of occludin at tight junctions. *J Cell Biol* **127:**1617-26

Furuse, M., Sasaki, H., Fujimoto, K., Tsukita, S. 1998. A single gene product, claudin-1 or -2, reconstitutes tight junction strands and recruits occludin in fibroblasts. *J Cell Biol* **143:**391-401

Furuse, M., Sasaki, H., Tsukita, S. 1999. Manner of interaction of heterogeneous claudin species within and between tight junction strands. *J Cell Biol* **147:**891-903

Gloushankova, N.A. 2008. Changes in regulation of cell-cell adhesion during tumor transformation. *Biochemistry (Mosc)* **73:**742-50

Gonzalez-Mariscal, L., Hernandez, S., Vega, J. 2008. Inventions designed to enhance drug delivery across epithelial and endothelial cells through the paracellular pathway. *Recent Pat Drug Deliv Formul* **2:**145-76

Gonzalez-Mariscal, L., Nava, P., Hernandez, S. 2005. Critical role of tight junctions in drug delivery across epithelial and endothelial cell layers. *J Membr Biol* **207:**55-68

Hamazaki, Y., Itoh, M., Sasaki, H., Furuse, M., Tsukita, S. 2002. Multi-PDZ domain protein 1 (MUPP1) is concentrated at tight junctions through its possible interaction with claudin-1 and junctional adhesion molecule. *J Biol Chem* **277:**455-61

Hartsock, A., Nelson, W.J. 2008. Adherens and tight junctions: structure, function and connections to the actin cytoskeleton. *Biochim Biophys Acta* **1778:**660-9

Hecht, G., Pothoulakis, C., LaMont, J.T., Madara, J.L. 1988. Clostridium difficile toxin A perturbs cytoskeletal structure and tight junction permeability of cultured human intestinal epithelial monolayers. *J Clin Invest* **82:**1516-24

Hou, J., Gomes, A.S., Paul, D.L., Goodenough, D.A. 2006. Study of claudin function by RNA interference. *J Biol Chem* **281:**36117-23

Itoh, M., Furuse, M., Morita, K., Kubota, K., Saitou, M., Tsukita, S. 1999. Direct binding of three tight junction-associated MAGUKs, ZO-1, ZO-2, and ZO-3, with the COOH termini of claudins. *J Cell Biol* **147:**1351-63

Itoh, M., Nagafuchi, A., Yonemura, S., Kitani-Yasuda, T., Tsukita, S. 1993. The 220-kD protein colocalizing with cadherins in non-epithelial cells is identical to ZO-1, a tight junction-associated protein in epithelial cells: cDNA cloning and immunoelectron microscopy. *J Cell Biol* **121:**491-502

Itoh, M., Sasaki, H., Furuse, M., Ozaki, H., Kita, T., Tsukita, S. 2001. Junctional adhesion molecule (JAM) binds to PAR-3: a possible mechanism for the recruitment of PAR-3 to tight junctions. *J Cell Biol* **154:**491-7

Jou, T.S., Schneeberger, E.E., Nelson, W.J. 1998. Structural and functional regulation of tight junctions by RhoA and Rac1 small GTPases. *J Cell Biol* **142:**101-15

Just, I., Fritz, G., Aktories, K., Giry, M., Popoff, M.R., Boquet, P., Hegenbarth, S., von Eichel-Streiber, C. 1994. Clostridium difficile toxin B acts on the GTP-binding protein Rho. *J Biol Chem* **269:**10706-12

Kapus, A., Szaszi, K. 2006. Coupling between apical and paracellular transport processes. *Biochem Cell Biol* **84:**870-80

Kniesel, U., Wolburg, H. 2000. Tight junctions of the blood-brain barrier. *Cell Mol Neurobiol* **20:**57-76

Liang, T.W., DeMarco, R.A., Mrsny, R.J., Gurney, A., Gray, A., Hooley, J., Aaron, H.L., Huang, A., Klassen, T., Tumas, D.B., Fong, S. 2000. Characterization of huJAM: evidence for involvement in cell-cell contact and tight junction regulation. *Am J Physiol Cell Physiol* **279:**C1733-43

Madara, J.L. 1989. Loosening tight junctions. Lessons from the intestine. *J Clin Invest* **83:**1089-94

Madara, J.L. 1998. Regulation of the movement of solutes across tight junctions. *Annu Rev Physiol* **60:**143-59

Madara, J.L., Barenberg, D., Carlson, S. 1986. Effects of cytochalasin D on occluding junctions of intestinal absorptive cells: further evidence that the cytoskeleton may influence paracellular permeability and junctional charge selectivity. *J Cell Biol* **102:**2125-36

Malergue, F., Galland, F., Martin, F., Mansuelle, P., Aurrand-Lions, M., Naquet, P. 1998. A novel immunoglobulin superfamily junctional molecule expressed by antigen presenting cells, endothelial cells and platelets. *Mol Immunol* **35:**1111-9

Martin, J., Malreddy, P., Iwamoto, T., Freeman, L.C., Davidson, H.J., Tomich, J.M., Schultz, B.D. 2009. NC-1059, a channel-forming peptide modulates drug delivery across in vitro corneal epithelium. *Invest Ophthalmol Vis Sci*

Matter, K., Balda, M.S. 2003. Signalling to and from tight junctions. *Nat Rev Mol Cell Biol* **4:**225-36

Matthews, J.B., Tally, K.J., Smith, J.A., Awtrey, C.S. 1994. F-actin differentially alters epithelial transport and barrier function. *J Surg Res* **56:**505-9

McCarthy, K.M., Francis, S.A., McCormack, J.M., Lai, J., Rogers, R.A., Skare, I.B., Lynch, R.D., Schneeberger, E.E. 2000. Inducible expression of claudin-1-myc but not occludin-VSV-G results in aberrant tight junction strand formation in MDCK cells. *J Cell Sci* **113 Pt 19:**3387-98

Mitic, L.L., Anderson, J.M. 1998. Molecular architecture of tight junctions. *Annu Rev Physiol* **60:**121-42

Miyoshi, J., Takai, Y. 2008. Structural and functional associations of apical junctions with cytoskeleton. *Biochim Biophys Acta* **1778:**670-91

Muresan, Z., Paul, D.L., Goodenough, D.A. 2000. Occludin 1B, a variant of the tight junction protein occludin. *Mol Biol Cell* **11:**627-34

Nusrat, A., Brown, G.T., Tom, J., Drake, A., Bui, T.T., Quan, C., Mrsny, R.J. 2005. Multiple protein interactions involving proposed extracellular loop domains of the tight junction protein occludin. *Mol Biol Cell* **16:**1725-34

Nusrat, A., Giry, M., Turner, J.R., Colgan, S.P., Parkos, C.A., Carnes, D., Lemichez, E., Boquet, P., Madara, J.L. 1995. Rho protein regulates tight junctions and perijunctional actin organization in polarized epithelia. *Proc Natl Acad Sci U S A* **92:**10629-33

Ogita, H., Ikeda, W., Takai, Y. 2008. Roles of cell adhesion molecules nectin and nectin-like molecule-5 in the regulation of cell movement and proliferation. *J Microsc* **231:**455-65

Reddy, G.L., Iwamoto, T., Tomich, J.M., Montal, M. 1993. Synthetic peptides and four-helix bundle proteins as model systems for the pore-forming structure of channel proteins. II. Transmembrane segment M2 of the brain glycine receptor is a plausible candidate for the pore-lining structure. *J Biol Chem* **268:**14608-15

Resink, T.J., Philippova, M., Joshi, M.B., Kyriakakis, E., Erne, P. 2009. Cadherins and cardiovascular disease. *Swiss Med Wkly* **139:**122-34

Roh, M.H., Liu, C.J., Laurinec, S., Margolis, B. 2002. The carboxyl terminus of zona occludens-3 binds and recruits a mammalian homologue of discs lost to tight junctions. *J Biol Chem* **277:**27501-9

Roura, S., Miravet, S., Piedra, J., Garcia de Herreros, A., Dunach, M. 1999. Regulation of E-cadherin/Catenin association by tyrosine phosphorylation. *J Biol Chem* **274:**36734-40

Rudini, N., Dejana, E. 2008. Adherens junctions. *Curr Biol* **18:**R1080-2

Saitou, M., Fujimoto, K., Doi, Y., Itoh, M., Fujimoto, T., Furuse, M., Takano, H., Noda, T., Tsukita, S. 1998. Occludin-deficient embryonic stem cells can differentiate into polarized epithelial cells bearing tight junctions. *J Cell Biol* **141:**397-408

Saitou, M., Furuse, M., Sasaki, H., Schulzke, J.D., Fromm, M., Takano, H., Noda, T., Tsukita, S. 2000. Complex phenotype of mice lacking occludin, a component of tight junction strands. *Mol Biol Cell* **11:**4131-42

Salama, N.N., Eddington, N.D., Fasano, A. 2006. Tight junction modulation and its relationship to drug delivery. *Adv Drug Deliv Rev* **58:**15-28

Schneeberger, E.E., Lynch, R.D. 2004. The tight junction: a multifunctional complex. *Am J Physiol Cell Physiol* **286:**C1213-28

Sept, D., McCammon, J.A. 2001. Thermodynamics and kinetics of actin filament nucleation. *Biophys J* **81:**667-74

Shen, L., Turner, J.R. 2005. Actin depolymerization disrupts tight junctions via caveolae-mediated endocytosis. *Mol Biol Cell* **16:**3919-36

Somasekharan, S., Brandt, R., Iwamoto, T., Tomich, J.M., Schultz, B.D. 2008. Epithelial barrier modulation by a channel forming peptide. *J Membr Biol* **222:**17-30

Stevenson, B.R., Begg, D.A. 1994. Concentration-dependent effects of cytochalasin D on tight junctions and actin filaments in MDCK epithelial cells. *J Cell Sci* **107 (Pt 3):**367-75

Stevenson, B.R., Siliciano, J.D., Mooseker, M.S., Goodenough, D.A. 1986. Identification of ZO-1: a high molecular weight polypeptide associated with the tight junction (zonula occludens) in a variety of epithelia. *J Cell Biol* **103:**755-66

Tai, C.Y., Kim, S.A., Schuman, E.M. 2008. Cadherins and synaptic plasticity. *Curr Opin Cell Biol* **20:**567-75

Tomich, J.M., Wallace, D., Henderson, K., Mitchell, K.E., Radke, G., Brandt, R., Ambler, C.A., Scott, A.J., Grantham, J., Sullivan, L., Iwamoto, T. 1998. Aqueous solubilization of transmembrane peptide sequences with retention of membrane insertion and function. *Biophys J* **74:**256-67

Tsukita, S., Furuse, M., Itoh, M. 2001. Multifunctional strands in tight junctions. *Nat Rev Mol Cell Biol* **2:**285-93

Umeda, K., Matsui, T., Nakayama, M., Furuse, K., Sasaki, H., Furuse, M., Tsukita, S. 2004. Establishment and characterization of cultured epithelial cells lacking expression of ZO-1. *J Biol Chem* **279:**44785-94

Van Itallie, C.M., Anderson, J.M. 2004. The role of claudins in determining paracellular charge selectivity. *Proc Am Thorac Soc* **1:**38-41

Van Itallie, C.M., Anderson, J.M. 2006. Claudins and epithelial paracellular transport. *Annu Rev Physiol* **68:**403-29

Van Itallie, C.M., Holmes, J., Bridges, A., Gookin, J.L., Coccaro, M.R., Proctor, W., Colegio, O.R., Anderson, J.M. 2008. The density of small tight junction pores varies among cell types and is increased by expression of claudin-2. *J Cell Sci* **121:**298-305

Wallace, D.P., Tomich, J.M., Iwamoto, T., Henderson, K., Grantham, J.J., Sullivan, L.P. 1997. A synthetic peptide derived from glycine-gated Cl- channel induces transepithelial Cl- and fluid secretion. *Am J Physiol* **272:**C1672-9

Wong, V., Gumbiner, B.M. 1997. A synthetic peptide corresponding to the extracellular domain of occludin perturbs the tight junction permeability barrier. *J Cell Biol* **136:**399-409

Yamamoto, T., Harada, N., Kano, K., Taya, S., Canaani, E., Matsuura, Y., Mizoguchi, A., Ide, C., Kaibuchi, K. 1997. The Ras target AF-6 interacts with ZO-1 and serves as a peripheral component of tight junctions in epithelial cells. *J Cell Biol* **139:**785-95

Yu, A.S., McCarthy, K.M., Francis, S.A., McCormack, J.M., Lai, J., Rogers, R.A., Lynch, R.D., Schneeberger, E.E. 2005. Knockdown of occludin expression leads to diverse phenotypic alterations in epithelial cells. *Am J Physiol Cell Physiol* **288:**C1231-41

CHAPTER 2 - p1130, A Synthetic Channel-forming Peptide and Derivatives Modulate Transepithelial Electrical Conductance across MDCK cell monolayers

Abstract

The goal of this study is to test the biological activities of p1130 derivates p1171, p1172 and p1173. Ussing chamber data suggested that apical exposure to p1171 increased short circuit current but did not influence transepithelial electrical conductance. The treatment of p1172 and p1173 increased short circuit current as well as conductance. These outcomes indicate that these p1130 derivates have channel-forming potentials across epithelial monolayers.

Introduction

M2GlyR (P-A-R-V-G-L-G-I-T-T-V-L-T-M-T-T-Q-S-S-G-S-R-A) is a synthetic peptide based on the second transmembrane of the GlyR α1 subunit. Existing evidences suggest that when exposed to the apical aspect of epithelial cells, M2GlyR incorporates with the cell membrane and undergoes supramolecular assembly to form anion-selective channels. However, M2GlyR has a low aqueous solubility as well as a propensity to aggregate in aqueous environment. These shortcomings limit the clinical application of M2GlyR as a potential treatment for cystic fibrosis. Therefore, more than 200 M2GlyR derived peptides were synthesized to optimize the peptide for clinical purpose by achieving higher aqueous solubility, lower solution associations as well as high anion selectivity.

Peptide p1130 (K-K-K-K-P-A-R-V-G-L-G-I-T-T-V-L-T-M-R-T-Q-W) is unique among the sequences derived from M2GlyR in that it appears to exhibit high aggregate conductivity, but virtually no anion to cation selectivity. Therefore, it is used as a platform for additional amino acid substitutions aimed at restoring anion selectivity. Modifications have been introduced to

alter pore residue electrostatics and pore length resulting in 3 sequences that provide the basis for outcomes presented in this chapter.

Peptide p1171 (p1130-T13Dap, T17Dap: K-K-K-K-P-A-R-V-G-L-G-I-Dap-T-V-L-Dap-M-R-T-Q-W), a peptide in which threonines (T) in p1130 are substituted by the diaminopropionic acid (L-Dap) at positions T13 and T17, was synthesized to study how electrostatics of pore lining residues affect assembly in cell membranes. Dap is a positively charged amino acid while T is polar yet uncharged. The introduction of two positive charges into the middle of a transmembrane sequence could prevent or reduce membrane insertion of this sequence. Before other *Bis*-Dap sequences are prepared it is important to determine whether the sequence produced a functional ion channel.

Two other sequences, p1172 (p1130- Ω ILTG -p26: K-K-K-K-P-A-R-V-G-L-G-I-L-T-G-I-T-T-V-L-T-M-R-T-Q-W) and p1173 (p1130- Ω LTGILTG -p29: K-K-K-K-P-A-R-V-G-L-G-L-T-G-I-L-T-G-I-T-T-V-L-T-M-R-T-Q-W), were synthesized to test for the effect of pore length on transepithelial ion flux. Modeling studies by Jianhan Chen suggested that the p1130 sequence caused a thinning of the lipid bilayer while these two peptides addressed the issue of pore length by adding one and two internal helical turns to p1130, respectively. Therefore, by inserting these helical turns in the positions indicated, the registry of the pore lining residues was maintained while lengthening the transmembrane segment. In this study the ability of these new sequences to insert into the membrane and then form functioning channel assemblies was tested.

Methods

Peptide Synthesis: All peptides were synthesized using solid-phase synthesis employing an automated base-labile 9-fluorenylmethyloxycarbonyl (Fmoc) strategy as described (Wallace et al., 1997b). Prepared peptides were purified to homogeneity by reverse-phase HPLC and analyzed by matrix-assisted laser desorption time of flight mass spectroscopy (Broughman et al., 2002a). The sequences of the peptides tested in this experiment are as follows:

p1171: K-K-K-K-P-A-R-V-G-L-G-I-Dap-T-V-L-Dap-M-R-T-Q-W
p1172: K-K-K-K-P-A-R-V-G-L-G-I-L-T-G-I-T-T-V-L-T-M-R-T-Q-W
p1173: K-K-K-K-P-A-R-V-G-L-G-L-T-G-I-L-T-G-I-T-T-V-L-T-M-R-T-Q-W

Chemicals: 1-EBIO (1-ethyl-2-benzimidazolinone; Acros, Pittsburgh, PA) was prepared as 1 M stock solution in dimethyl sulfoxide. Forskolin (*Coleus forskohlii*; Calbiochem, La Jolla, CA) was prepared as 10 mM stock in ethanol. Peptide stock solutions of 5 mM, calculated based on the theoretical molecular weight of synthetic peptides, were prepared in deionized water just prior to use. Unless otherwise noted, all other reagents were purchased from Sigma Chemical (St. Louis, MO).

Cell culture: MDCK (Madin-Darby canine kidney) cells were obtained from Dr. Lawrence Sullivan (University of Kansas Medical Center, Kansas City, KS). The culture medium was a 1:1 mixture of Dulbecco's Modified Eagle Medium and Nutrient F12 (GIBCO, Invitrogen, Carlsbald, CA), 5% heat inactivated fetal bovine serum (Atlanta Biologicals, Atlanta, GA) and 1% penicillin and streptomycin as described previously (Broughman et al., 2001). The media were refreshed every alternate day. Cells were maintained on plastic 25-cm^2 cell culture flasks (Corning Inc., corning, NY) in a humidified environment with 5% CO_2 at 37˚C and passaged every 3-4 days after growing to 90 to 100% confluence, treated with 0.25% trypsin and 2.6 mM EDTA (GIBCO) and dispersed using gentle mechanical force to dislodge the cells from cell culture flask surface. For the Ussing chamber experiments, approximately 2.5 x 10^5 cells were seeded onto 1.13 cm^2 permeable supports (Snapwell, 12-mm diameter, Costar, Corning Inc.) 14 days prior to experimental evaluation.

Electrophysiology: Transepithelial ion transport was measured using a modified Ussing chamber (model DCV9, Navicyte, San Diego, CA) as described previously (Broughman et al., 2004; Broughman et al., 2001). For typical electrical ion flux measurements, monolayers were bathed symmetrically in Ringer solution (120 mM NaCl, 25 mM $NaHCO_3$, 3.3 mM KH_2PO_4, 0.8 mM K_2HPO_4, 1.2 mM $MgCl_2$, and 1.2 mM $CaCl_2$; ～290 mOsmol/kg H_2O) prepared just before use, maintained at 37˚C and continuously bubbled with 5% CO_2/ 95% O_2 to provide mixing and pH stability. The monolayers were clamped to 0 mV and a 5 s 1 mV bipolar pulse was generated automatically every 100 s using a voltage clamp (model 558C-5, University of Iowa, Dept. of Bioengineering, Iowa City, IA). The current change in response to the voltage pulse was used to calculate transepithelial conductance (g_{te}) according to Ohm's law ($g_{te} = 1/R_{te}=\Delta I/\Delta V$). Data were acquired at 1 Hz with an Intel based computer using an MP100A-CE interface and AcqKnowledge software (version 3.7.3, BIOPAC Systems, Santa Barbara, CA).

Data analysis: All numerical results are reported as mean ± SEM. All graphs and regression fits were completed using Sigmaplot 2000 (v 10.0, Systat Software Inc, San Jose, CA) and/or Excel (v 11.8, Microsoft Corp, Redmond, WA).

Results

Channel-Forming Potential

Experiments were conducted to determine whether these synthesized peptides displayed channel-forming activity, as indicated by an increase in short circuit current (I_{sc}). Fig 2.1 shows the recordings from typical experiments in which MDCK monolayers were exposed to synthetic peptides at two different concentrations, 30 μM and 100 μM.

MDCK epithelial cell monolayers with low basal g_{te} (1.0 ± 0.1 mS cm^{-2}) and low basal I_{sc} (0.39 ± 0.04 μA cm^{-2}), were pretreated with 300 μM 1-EBIO, an activator of Ca^{2+}- dependent basolateral K^+ channels IK and SK, to hyperpolarize the cells and maximize the electrochemical driving force for anion secretion (Broughman et al., 2004; Devor et al., 1996). Exposure of MDCK monolayers to 1-EBIO resulted in peak I_{sc} of 1.07 ± 0.09 μA cm^{-2} with a slight sustained increase in I_{sc} of 0.67 ± 0.07 μA cm^{-2} as well as a slightly increase in g_{te} of 0.23 ± 0.18 mS cm^{-2}. The changes of I_{sc} were consistent with the activation role of 1-EBIO. The modest effect of 1-EBIO suggested that the basolateral membrane in MDCK monolayers was not rate limiting for anion secretion. After reaching the peak elicited by 1-EBIO, the I_{sc} decreased towards basal I_{sc} and attained a value of 0.75 ± 0.09 μA cm^{-2} after ~ 5 minutes.

After the pretreatment of 1-EBIO, peptide p1171 dissolved in distilled water with concentrations of 30 μM and 100 μM were added to the apical surface of polarized MDCK monolayers (Fig 2.1A). Treatment with 30 μM p1171 resulted in a rapid increase of 1.80 ± 0.63 μA cm^{-2} in I_{sc} within 3 minutes. Similar with 30 μM p1171 treatments, exposure to 100 μM p1171 caused an immediate increase of 2.11 ± 0.33 μA cm^{-2} in I_{sc}. After reaching its I_{sc} peak in less than 3 minutes, the I_{sc} declined to a value of 1.06 ± 0.29 μA cm^{-2} after more than 16 minutes. The summary data from 3-5 observations suggested that there was no significant difference between two concentrations when comparing the p1171 elicited I_{sc} changes (Fig 2.1D).

Exposure of the MDCK monolayers to either p1172 (Fig 2.1B) or p1173 (Fig 2.1C) was associated with rapid increases in I_{sc} that reach peak values in a concentration dependent manner before declining. Apical exposure to p1172 at 30 μM caused an increase in I_{sc} from 0.68 ± 0.11

μA cm^{-2} to 3.21 ± 0.65 μA cm^{-2} in 3 minutes, and then started to decline to baseline but remained at 1.73 ± 0.19 μA cm^{-2} after more than 16 minutes. Apical exposure to 100 μM p1172 also resulted in an immediate increase in I_{sc} followed by declining to a higher residual I_{sc} after the same time course. From Fig 2.1D, it was obvious that the effect of 100 μM p1172 on I_{sc} was nearly 2 folds of the effect of 30 μM p1172. Like p1172, peptide p1173 also elicited instant increase in I_{sc} at concentrations 30 μM and 100 μM. After peak I_{sc}, the I_{sc} declined toward peptide pre-treatment level but remained at an elevated I_{sc} value. The concentration dependent effect of peptide p1173 was much greater than p1172. The treatment of 100 μM p1173 caused more than 4 fold I_{sc} change than 30 μM p1173 (Fig 2.1D). Meanwhile, there is significant difference between I_{sc} changes caused by 100 μM p1172 and 100 μM p1173. It indicates that the ion channel forming potential of p1172 and p1173 might be different.

All MDCK epithelial monolayers responded to forskolin after the effect of the peptides had diminished. Forskolin is an adenylyl cyclase activator that induces the conversion of ATP to cAMP, which activates protein kinase A. Protein kinase A activates components of active ion transport pathways, such as CFTR, which ultimately results in increased anion secretion (Carlin et al., 2006; Hedin & Rosberg, 1983). In these MDCK monolayers, the addition of 2 μM forskolin resulted in a rapid transient ΔI_{sc} of 22.19 ± 1.22 μA cm^{-2}. After the I_{sc} peak, there followed a plateau which indicates ongoing anion secretion (data not shown). The I_{sc} changes caused by forskolin suggested that MDCK monolayers were still viable and responsive to cAMP-mediated stimulation after the exposure to these peptides.

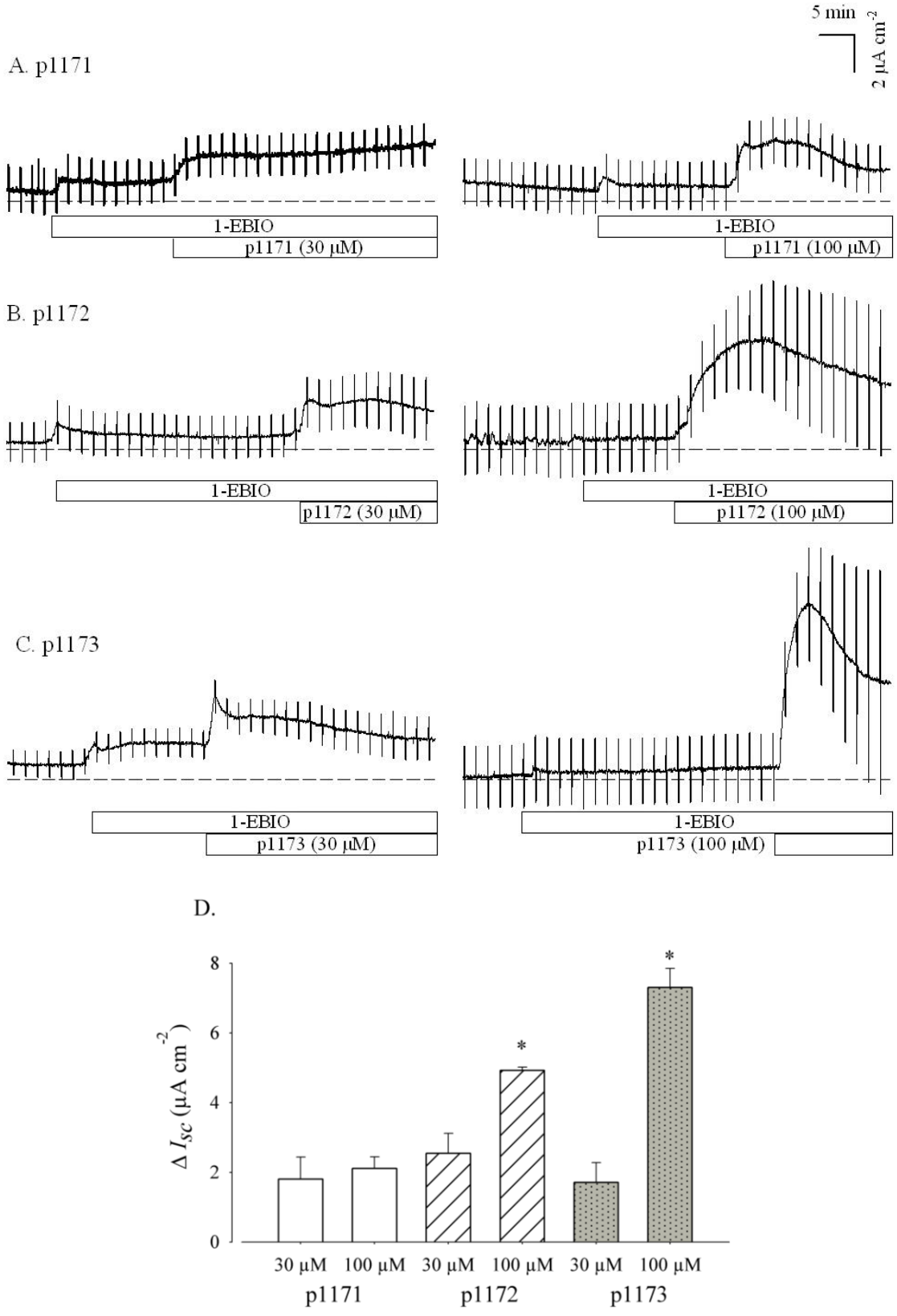

Figure 2.1 Synthesized peptides induce elevation in short circuit current across MDCK monolayers.

A-C) Representative traces of I_{sc} measured from MDCK monolayers exposed to 1-EBIO and apically to synthesized peptides p1171, p1172 and p1173, as indicated. The dashed line represents the reference point of zero, indicating no net flux of ions.

D) Summarized results of synthesized peptides induced I_{sc} change for n=3-5 (± SEM).

Asterisk (*) indicates significant difference between ΔI_{sc} caused by different concentrations.

Conductance change

The magnitude of the current change caused by bipolar voltage pulses was used to calculate the changes in g_{te} over time. All MDCK monolayers tested had a low basal g_{te} of 0.98 ± 0.10 mS cm^{-2} and their g_{te} increased to 1.24 ± 0.18 mS cm^{-2} after the pretreatment of 1-EBIO.

The g_{te} did not change significantly after exposure to p1171, at either concentration tested (Fig 2.1A). As opposed to p1171, exposure to peptides p1172 and p1173 showed a definite increase in g_{te} associated with changes in I_{sc}.

Different from I_{sc}, which reached peak value within 3 minutes after apical exposure of 30 µM and 100 µM p1172, the g_{te} usually began to increase after reaching the peak I_{sc}, even continuing to increase during the decline of I_{sc} and generally reaching a maximum value after exposure to peptide for ~ 30 minutes. For peptide p1172, the maximal value of g_{te} at 100 µM was 3.23 ± 0.75 mS cm^{-2}, which was more than two-fold of the maximal value of g_{te} at 30 µM, 1.33 ± 0.28 mS cm^{-2} (Fig 2.2A).

The conductance increase caused by 30 µM and 100 µM p1173, was similar to p1172 described above. However the concentration-dependent effect appeared to be more substantial for peptide p1173. The maximal value of g_{te} at 100 µM was 3.79 ± 1.05 mS cm^{-2} while the maximal value of g_{te} at 30 µM was 1.04 ± 0.13 mS cm^{-2} (Fig 2.2B). The much slower onset of Δg_{te} than ΔI_{sc} suggests that there might be different pathways regulated by synthetic peptides to account for these different outcomes.

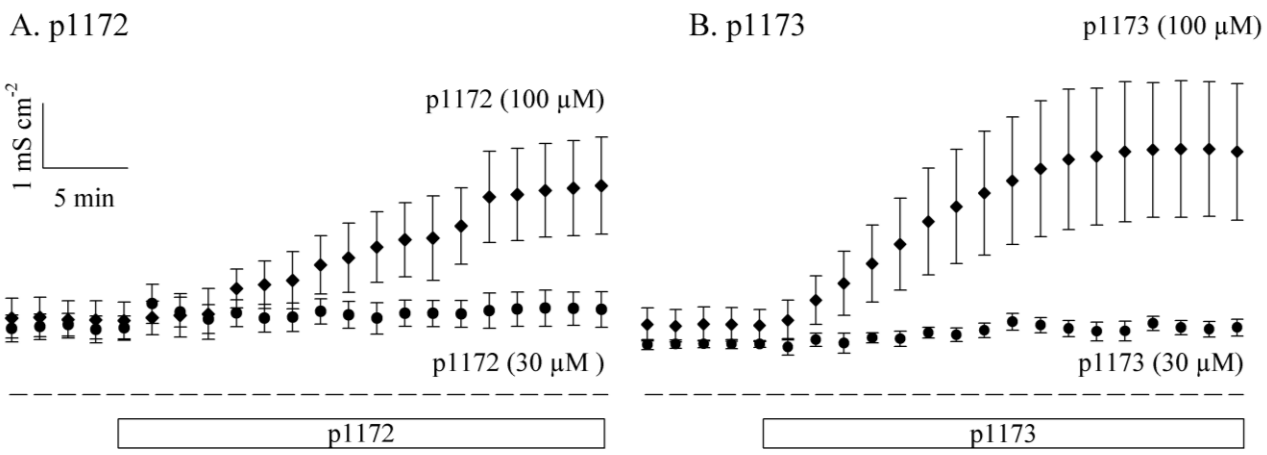

Figure 2.2 Synthesized peptides p1172 and p1173 cause a concentration- and time- dependent elevation in conductance (g_{te}) across MDCK monolayers.

A) Peptide p1172 and B) peptide p1173 treatments caused concentration dependent increases in conductance with a much slower onset than the increase in short circuit current. n=3-5 (± SEM)

Discussion

The results suggested that p1130 derivatives p1171, p1172 or p1173 can form functional ion channels in the apical membranes of MDCK cells grown as monolayer cultures.

Peptide p1171 is a doubly substituted peptide of p1130. The uncharged amino acid threonine at positions T13 and T17 in NC-1130 were both replaced by the amino acid diaminopropionic acid (R_{group}= —CH_2—NH_3^+, which has a net positive charge at physiological pH). The addition of cation residues to the transmembrane sequence might potentially interfere with the membrane insertion and assembly steps. Therefore, electrophysiological experiments were conducted to examine whether p1171 still have an ion channel forming potential.

The doubly substituted peptide p1171 induced a rapid increase in I_{sc}, which suggests that after cationic amino acids replacement, the peptide can still form stable ion-conducting pores. However, there is no big difference between ΔI_{sc} caused by 30 μM and 100 μM. According to Hill equation, when the concentration of substrate is much higher than the apparent K_d, then the reaction rate will be affected by concentration. It is possible that at a concentration of 30 μM, ΔI_{sc} has already reached its maximal value. Therefore, 100 μM will be expected to have the same effect on $I_{sc.}$ It is also possible that the concentrations at 30 μM and 100 μM are too low from a working concentration of p1171 to cause a difference effect on ΔI_{sc} across MDCK monolayers. Further experiments can be done by testing lower concentrations (100 pM, 300 pM, 1 μM) and higher concentrations (1 mM, 3 mM, 10 mM) of p1171 to determine the complete concentration dependency.

Peptide p1172 is formed by adding a four-residue sequence ILTG to NC-1130 while peptide p1173 is formed by adding a seven residue sequence ILTGILT. The channel-forming sequence p1130 induces an apparent thinning of the membrane according to computer modeling. Membrane thinning has been observed with a number of pore-forming antimicrobial peptides and it seems to be a general phenomenon associated with pore formation (Huang, 2006; Jang, et al., 2006).

The increases in I_{sc} after exposure to either p1172 or p1173 suggest that either peptide can increase ion transport and elicit anion secretion or cation absorption. Compared with p1130, which has 22 amino acids and whose membrane spanning length is 18 amino acids, peptide p1172 with one more helical turn elicited higher *Isc* change and g_{te} change. And the longest

sequence discussed here, p1173, which is predicted to have two more helical turns than p1130, had the highest effect in I_{sc} and g_{te} in all three peptides. Meanwhile, the elevations of g_{te} suggest that synthesized peptides p1172 and p1173 might modulate epithelial transport, and possibly through the paracellular route.

The peptide p1130 is remarkable in several ways: **1)** it is small and easily synthesized; **2)** it is water soluble and can be delivered to membrane surfaces without the need of added organic solvents; **3)** it is predominantly monomeric in solution; **4)** when inserted into membranes it orients in the same direction due to the highly positively charged N-terminus; **5)** the pore form through self-association contains helices in a parallel orientation; **6)** functional ion conducting pores are formed that can provide information on various channel properties; and **7)** the small size of the peptide and the assembled pore facilitates both structural analyses and computer modeling that can produce informative structures. All three derivatives of p1130, peptides p1171, p1172, p1173 showed ion channel forming potential. Further study might focus on P_{Cl}/P_{Na} and P_{Cl}/P_{K} to define the exact value of anion selectivity of these synthetic peptides in order to determine whether changing pore residue electrostatics and changing pore length would increase anion selectivity of p1130. Our final purpose is try to find a p1130 derivative with all the original advantages of p1130 as well as higher anion to cation selectivity, this sequence would be ideal for enhancing apical Cl^- conductance and can be served as a substitute for endogenous Cl^- channels for the treatment of cystic fibrosis.

References

Broughman, J.R., Brandt, R.M., Hastings, C., Iwamoto, T., Tomich, J.M., Schultz, B.D. 2004. Channel-forming peptide modulates transepithelial electrical conductance and solute permeability. *Am J Physiol Cell Physiol* **286:**C1312-23

Broughman, J.R., Mitchell, K.E., Sedlacek, R.L., Iwamoto, T., Tomich, J.M., Schultz, B.D. 2001. NH(2)-terminal modification of a channel-forming peptide increases capacity for epithelial anion secretion. *Am J Physiol Cell Physiol* **280:**C451-8

Broughman, J.R., Shank, L.P., Prakash, O., Schultz, B.D., Iwamoto, T., Tomich, J.M., Mitchell, K. 2002. Structural implications of placing cationic residues at either the NH2- or COOH-terminus in a pore-forming synthetic peptide. *J Membr Biol* **190:**93-103

Carlin, R.W., Sedlacek, R.L., Quesnell, R.R., Pierucci-Alves, F., Grieger, D.M., Schultz, B.D. 2006. PVD9902, a porcine vas deferens epithelial cell line that exhibits neurotransmitter-stimulated anion secretion and expresses numerous HCO3(-) transporters. *Am J Physiol Cell Physiol* **290:**C1560-71

Devor, D.C., Singh, A.K., Frizzell, R.A., Bridges, R.J. 1996. Modulation of Cl- secretion by benzimidazolones. I. Direct activation of a Ca(2+)-dependent K+ channel. *Am J Physiol* **271:**L775-84

Hedin, L., Rosberg, S. 1983. Forskolin effects on the cAMP system and steroidogenesis in the immature rat ovary. *Mol Cell Endocrinol* **33:**69-80.

Huang H.W. (2006) Molecular mechanism of antimicrobial peptides: the origin of cooperativity. *Biochim Biophys Acta*. **1758**(9):1292-1302.

Jang H, Ma B, Woolf TB, Nussinov R. (2006) Interaction of protegrin-1 with lipid bilayers: membrane thinning effect. *Biophys J*. **91**:2848-2859.

Wallace, D.P., Tomich, J.M., Iwamoto, T., Henderson, K., Grantham, J.J., Sullivan, L.P. 1997. A synthetic peptide derived from glycine-gated Cl- channel induces transepithelial Cl- and fluid secretion. *Am J Physiol* **272:**C1672-9

CHAPTER 3 - NC-1059, a Channel-Forming Peptide Reversibly Modulates Epithelial Paracellular Pathway

Suma Somasekharan[1], Sheng Yi[1], Takeo Iwamoto[1], John M. Tomich[1], and Bruce D. Schultz[2]

Departments of [1]Biochemistry and [2]Anatomy and Physiology
Kansas State University, Manhattan, KS 66506

Corresponding author: Dr. Bruce D. Schultz
Department of Anatomy and Physiology
1600 Denison Avenue, Coles Hall 228
Manhattan, KS-66506
Phone numbers: 785-532-4839 (office), 785-532-4557 (fax).
Email: bschultz@vet.ksu.edu
Running title: NC-1059 Modulates Epithelial Paracellular Pathway

A previous version of this chapter was included as a part of Dr. Suma Somasekharan's PhD thesis that is available through Kansas State University libraries ("NC-1059, a Channel Forming Peptide, Induces a Reversible Change in Barrier Function of Epithelial monolayers", 2008, p83-124, available at http://hdl.handle.net/2097/553). The chapter included in Dr. Somasekharan's thesis was submitted to a journal for peer review. Subsequently, the manuscript was revised substantially to address reviews' concerns. Additional experiments that constitute a substantial portion of the research project conducted to complete the master degree requirements were added to this chapter. New data were added to demonstrate that NC-1059 modulates F-actin:total actin ratio. New data were also added to rule out the possibilities that the change of tight junction permeability was caused by cell loss from the monolayer or caused by an effect on cell viability. Significant contributions were made to Figs 3.4, 3.5, 3.7, 3.9, 3.10, 3.13 and 3.14.

Abstract

The goal of this study is to determine cellular changes that account for increased epithelial paracellular permeability by NC-1059, a synthetic channel forming peptide. Apical exposure to NC-1059 (60 μM) was shown previously to increase short circuit current, transepithelial electrical conductance (g_{te}) and enhanced the permeation of 9.5 kDa dextran, but not 77 kDa dextran across MDCK monolayers, all of which returned to pretreatment levels within 48 hrs after removal of the peptide from the apical medium. MDCK monolayers in the present study showed a large increase in g_{te} and enhanced permeation of 40 and 70 kDa dextran when exposed to NC-1059 at greater concentrations (100 and 200 μM). Following exposure to NC-1059 for 60 min, epithelial monolayers showed a substantial recovery in g_{te} at 24 hrs and returned to pretreatment values within 48 hours. Immunolabeling and immunoblotting revealed an NC-1059 associated decrease in the F-actin to G-actin ratio and concentration dependent reorganization or loss of actin cytoskeleton, tight junction proteins ZO-1 and occludin and adherens junction proteins E-cadherin and β-catenin that occurred over a 15 to 60 min period. Effects of NC-1059 exposure were reversible with progressive recovery of immunoreactivity at the apical cell junction for occludin and ZO-1 observed 24 and 48 hrs post exposure. The modulation of the epithelial tight junctions in a reversible manner indicates that NC-1059 has therapeutic potential to increase the efficiency of drug delivery across barrier membranes.

Key words: Occludin, ZO-1, Actin, Paracellular permeability, Transepithelial conductance

Introduction

NK_4-M2GlyR (KKKKPARVGLGITTVLTMTTGSSGSRA) is a channel forming peptide that was synthesized by adding four lysine residues to the second transmembrane segment (M2) of the glycine receptor (GlyR) alpha-subunit (Broughman et al., 2001; Tomich et al., 1998; Wallace et al., 1997) and was shown to increase anion secretion by epithelial monolayers. However, the subsequent removal of up to five C-terminus residues from NK_4-M2GlyR reduced aggregation of the peptide in aqueous solution while retaining ion transport properties (Broughman et al., 2001). Based on the hypothesis that only the N-terminus half of the peptide was necessary for its ion transport properties, a palindromic peptide was designed with 11 residues from the N-terminal half of NK_4-M2GlyR. The final sequence, KKKKAARVGLGITTV LVTTIGLGVRAA, was termed NC-1059 (Broughman et al., 2004).

NC-1059 enhances ion transport and reduces barrier function of epithelial monolayers. MDCK monolayers that were exposed apically to NC-1059 showed a concentration dependent increase in short circuit current (I_{sc}), demonstrating an increase in anion secretion or cation absorption. The transepithelial electrical conductance (g_{te}), a measure of epithelial barrier function, also increased in a concentration dependent manner (Broughman et al., 2004). Similar outcomes have now been reported for epithelia derived from cornea (Martin et al., 2009), colon, airway, and reproductive duct (Somasekharan et al., 2008). Furthermore, NC-1059 enhanced dextran permeation across epithelial monolayers, showing that a paracellular route was opened (Broughman et al., 2004). The effect of the peptide on g_{te} and paracellular solute movement was reversed within 48 hrs of returning the monolayers to fresh culture medium. The cell monolayers regained responsiveness to subsequent treatments with the peptide (Broughman et al., 2004; Martin et al., 2009). Thus the effects of NC-1059 on epithelial monolayers are reversible and repeatable.

Epithelial cell layers act as barriers to the movement of hydrophilic or uncharged solutes. Tight junctions are multimolecular complexes located between the apical intercellular regions of epithelial cells that regulate paracellular permeability (Schneeberger & Lynch, 2004). Occludin, claudins, junctional adhesion molecule-1 (JAM-1) and zona occludens protein-1 (ZO-1), along with other proteins form the tight junctions (Schneeberger & Lynch, 2004). This tight junction complex associates with the perijunctional actomyosin ring and the complex is proposed to be

involved in regulation of solute movement through the paracellular route (Madara, 1998). Compounds such as bacterial and fungal toxins (e.g., *Clodtridium difficle* toxins, ochratoxin), positively charged molecules (e.g., protamine) and chitosans are amongst several molecules observed to cause an increase in g_{te} through an effect on actin organization and/or localization of junctional proteins (McLaughlin et al., 2004; Moore et al., 1990; Peixoto & Collares-Buzato, 2005; Schipper, Varum & Artursson, 1996). Peptides corresponding to the first and second extracellular loops of occludin also increased paracellular permeability, although several hrs were required to produce significant effects (Chung et al., 2001; Wong & Gumbiner, 1997). A modified occludin peptide reportedly enhanced permeability across airway epithelia and caused a loss in occludin localization at the tight junctions (Tavelin et al., 2003). *Vibrio cholerae* produces zonula occludens toxin (ZOT), a naturally occurring peptide that increases the permeability of small intestine epithelia (Fasano et al., 1997). ZOT is rapid in onset (<20 min) and the effects are reversible. ZOT causes reorganization of actin and a change in the localization of ZO-1 (Fasano et al., 1995). VP8, a rotavirus surface protein, enhances paracellular permeability by causing a redistribution of occludin, ZO-1 and claudin-3 at the tight junctions in MDCK monolayers (Nava et al., 2004). These results suggest that the actin cytoskeleton and proteins comprising the tight junctions can be modulated either in distribution or abundance to affect epithelial barrier function.

Adheren junctions also contribute to the epithelial barrier. E-cadherin is a transmembrane adheren junction protein that self associates in the extracellular space and associates with the actin cytoskeleton through β-catenin intracellularly. These interactions are important in maintaining cell morphology and are thought to be important for paracellular permeability (Hartsock & Nelson, 2008). Additionally, E-cadherin and β-catenin are important players in the assembly of the tight junctions (Gumbiner, 2005; Rajasekaran et al., 1996). Disruption of E-cadherin is associated with an increase in paracellular permeability with an associated change in actin organization and the organization of other junctional proteins (Wu et al., 1998; Wu et al., 2007; Wu et al., 2006). Hence, a pronounced reorganization in actin might involve a change in distribution of E-cadherin and β-catenin.

The focus of this study is to establish the molecular basis that accounts for NC-1059 enhancement of the permeability across MDCK monolayers. It was hypothesized that NC-1059 alters the localization of one or more junctional proteins. Also, since the actin cytoskeleton plays

a significant role in regulating paracellular permeability, NC-1059 was speculated to induce changes in permeability by altering actin organization. The outcomes show that NC-1059 exposure is associated with changes in both the abundance and localization of junctional proteins and that these effects were fully reversible in MDCK cells over 24-48 hours.

Methods

Peptide Synthesis: NC-1059 was synthesized as described previously by solid phase synthesis using 9-fluorenylmethoxycarbonyl chemistries (Broughman et al., 2002). The peptide was purified by reversed-phase HPLC and characterized by Edman degradation and matrix-assisted laser desorption time of flight mass spectroscopy (Broughman et al., 2002).

Chemicals: A 4% paraformaldehyde solution in phosphate buffered saline (PBS) was prepared from a 16% paraformaldehyde stock (Electron Microscopy Sciences, Hatfield, PA). Peptide stocks of 5 mM or 8 mM were prepared in deionized water just prior to use. Unless otherwise indicated, chemicals used were reagent grade obtained from Sigma Aldrich (St. Louis, MO).

Cell culture: MDCK cells were obtained from Dr. Lawrence Sullivan (University of Kansas Medical Center, Kansas City, KS) and grown in a medium containing a 1:1 mixture of Dulbecco's Modified Eagle Medium (DMEM) and Nutrient F12 (GIBCO, Invitrogen, Carlsbald, CA), 5% heat inactivated fetal bovine serum (FBS, Atlanta Biologicals, Atlanta, GA) and 1% penicillin and streptomycin as described previously (Broughman et al., 2004; Broughman et al., 2001). PVD9902 cells, epithelial cells derived from porcine vas deferens, were grown in a medium containing DMEM, 10% heat inactivated FBS and 1% penicillin and streptomycin as described previously (Carlin et al., 2006; Somasekharan et al., 2008). Cells were grown in plastic 25-cm^2 cell culture flasks (Corning, Inc., Coring, NY) in a humidified incubator with 5% CO_2 at 37ºC. Cultures that were >90% confluent were treated with 0.25% trypsin and 2.6 mM EDTA (GIBCO) and gentle mechanical force was used to dislodge cells from the surface. Approximately $2x10^5$ cells were seeded onto 1.13 cm^2 permeable supports (Snapwell, Costar, Corning Inc.) and cultured for 14 days prior to experimental evaluation. A tenth of the cells were also seeded onto flasks for further passages. The media were refreshed every alternate day.

Electrical Measurements: I_{sc} and transepithelial electrical potential were measured using a modified Ussing Chamber (model DCV9, Navicyte, San Diego, CA) as described previously (Broughman et al., 2004; Broughman et al., 2001). Monolayers were bathed symmetrically with Ringer solution (in mM: 120 NaCl, 25 $NaHCO_3$, 3.3 KH_2PO_4, 0.8 K_2HPO_4, 1.2 $MgCl_2$, and 1.2 $CaCl_2$) that was prepared fresh daily, maintained at 37ºC and bubbled with 5% CO_2-95% O_2 to achieve continuous mixing and to maintain pH. The monolayers were clamped to 0 mV and a 5 s

1 mV bipolar pulse was applied every 100 s using a voltage clamp (model 558C-5, University of Iowa, Dept. of Bioengineering, Iowa City, IA). Data acquisition was performed at 1 Hz using an Intel based computer and MP100A-CE interface (v. 3.2.6, BIOPAC Systems, Santa Barbara, CA). The current measured in response to the voltage pulse was used to calculate g_{te} (g_{te} = $\Delta I/\Delta V$).

FITC-Dextran permeability assay: Dextran permeation through the monolayer was measured as described previously (Broughman et al., 2004). The medium was removed and the monolayers were washed with warmed PBS. Ringer solution was added to the basolateral (1 ml) and apical (200 μl) compartments in the Snapwell culture plate. NC-1059 (200 μM) or vehicle was added to the Ringer solution on the apical side of the monolayers. Paired monolayers were exposed to 5 mM EDTA in hypotonic Ringer solution (50% dilution with water). Dextran (40 or 70 kDa) conjugated to FITC (0.5 mg) was added to the apical compartment of all treatments. After incubation at 37ºC for 1 hr samples were taken from the basolateral compartment for determination of fluorescence intensity (Fluorskan Ascent FL, Thermo Fisher Scientific, Waltham, MA). A series of dilutions of each size of dextran was prepared and fluorescence determined as a function of concentration. A linear regression was used to derive the slope and calculate the amount of dextran that permeated each monolayer.

Recovery experiments: Monolayers were mounted into modified Ussing chambers and I_{sc} and g_{te} measured as described. Monolayers were exposed to either 100 or 200 μM NC-1059 or vehicle (Ringer solution) for 60 min and returned to the incubator in the presence of fresh culture medium for either 24 or 48 hrs before g_{te} was assessed again. Monolayers were fixed subsequently with 4% paraformaldehyde and labeled with anti-occludin and anti-ZO-1 antibodies as described below.

Cell counting: MDCK cells grown to >90% confluent in plastic 25-cm^2 cell culture flasks were detached from the surface and adjacent cells by treating with 0.25% trypsin and 2.6 mM EDTA followed by gentle mechanical force. Cells were suspended in 1 ml cell culture medium and samples were loaded into the chamber of a hemacytometer (Hausser Scientific Company, PA) to determine cell density using darkfield microscopy (Nikon, Inc., Melville, NY). Approximately 3×10^4, 1×10^5, 3×10^5, 1×10^6 cells were seeded onto 1.13 cm^2 permeable supports and assessed in modified Ussing chambers after 24 and 48 hrs growth as described above.

Cell membrane integrity assay: Lactate dehydrogenase (LDH) is released from cells that have compromised membranes that is indicative of cell death. LDH activity was measured in medium bathing the apical aspect of MDCK cells using a commercially available fluorescence-based kit (CytoTox-ONE; Promega Corp., Madison, WI). LDH activity was assessed using MDCK cells grown on both solid supports as outlined for the best performance of the kit and using cells grown on permeable supports as is typical for assessment of ion transport and barrier function. In initial studies, MDCK cells were seeded onto sterile 96-well opaque-walled tissue culture plates (Nalge Nunc International Corp., Rochester, NY) at a density of 1×10^5 cells/well. After 72 hours, cells were treated with vehicle, NC-1059 (200 μM) or EDTA (5 mM) for 60 min. Lysis solution (2 μL) was added to cells in paired wells to determine maximal LDH release. LDH activity was measured fluorometrically according to the manufacturer's instructions with outcomes reported in arbitrary fluorescent units. Assays were conducted to verify that the rate of increase in fluorescence was linear over the 10 min duration of the incubation and that the rate of increase in fluorescence was proportional to the volume of supernatant used for the assay. Subsequently, experiments were conducted with MDCK cells grown on permeable supports for 14 days. Monolayers were washed with warmed PBS were treated with vehicle, NC-1059 or EDTA for 1 hour or with lysis solution to achieve maximal LDH release. Five μL of the apical medium was employed to determine LDH activity in each condition as described above.

Immunolabeling: MDCK monolayers were exposed to NC-1059 for 5, 15, 30 and 60 min. NC-1074 (KKKKARSGSSQTTMTLARSGSSQTTMT), a peptide that does not elicit changes in epithelial electrical parameters, or vehicle was used to verify specificity of the NC-1059 effects. Following exposure to peptide or vehicle, monolayers were fixed with 4% paraformaldehyde and then incubated with anti-occludin (Zymed, Carlsbad, CA) or anti-ZO-1 (Chemicon, Temecula, CA and Zymed) antibodies and with Alexa 488 conjugated phalloidin (Molecular Probes, Carlsbad, CA). In a third set of experiments, MDCK monolayers were exposed to vehicle or NC-1059 for 30 or 60 min. Monolayers were fixed subsequently and labeled with anti-E-cadherin (Hybridoma bank, University of Iowa, Iowa City, IA) or anti-β-catenin (BD Biosciences, San Jose, CA) antibodies. Secondary antibodies were conjugated to Alexa 488 (green), Alexa 594 (Red) or rhodamine (Red). TOPRO-3 (blue; Molecular Probes) was used to label the nucleus. Images were acquired using a confocal microscope (LSM 510, Carl Zeiss AG, Jena, Germany). Optical sections (0.8 μm) were obtained along the Z-axis from the apical to basolateral aspect of

the cells to make a Z-stack. Three-dimentional projection was used to obtain a composite view of selected regions within the Z-stack.

Immunoblotting: Proteins were extracted from MDCK monolayers following exposure to NC-1059 or vehicle. Monolayers were lysed using RIPA buffer (composition: 150 mM NaCl, 10 mM HEPES, 2 mM EDTA, 1% Triton X-100, 0.2% SDS, 0.5% sodium deoxycholate) with protease inhibitor cocktail III (Calbiochem, San Diego, CA) and Halt phosphatase inhibitor cocktail (Pierce, Rockford, IL), and the lysate was passed repeatedly through a 21 gauge needle. The lysate was incubated at 4ºC for 1 hr and then centrifuged at 4ºC and 14,000g for 15 min. The supernatant was collected and protein concentration determined using the bicinchoninic acid (BCA) method using albumin as the standard (Pierce). The supernatants were mixed with 5x Laemmli sample buffer (250 mM Tris base, 40% glycerol, 0.8% SDS, 20% β-mercaptoethanol and 0.01% bromophenol blue). Equal amounts of protein (15 to 35 μg) for each treatment were loaded onto 4-15% gels (Biorad, Hercules, CA) and resolved at a 140 mV for 1 hr in running buffer (25 mM Tris Base, 200 mM Glycine, 0.1 % SDS). Proteins were transferred onto Immobilon–P transfer membranes (Millipore, Billerica, MA) for four hrs at 50V with transblot buffer (25 mM Tris base, 192 mM glycine, 20% v/v methanol). The membranes were blocked with 5% blotting grade milk (Biorad) in TBS (20 mM Tris base, 0.8% NaCl, pH 7.6) with 0.1% Tween-20 for 2 hours. Subsequently, the membranes were probed with either anti-occludin Mab (BD Biosciences), anti-ZO-1 Mab (Zymed), anti-E-cadherin, anti-β-catenin or anti-GAPDH Mab (Abcam, Cambridge, MA). HRP-conjugated anti-rabbit and anti-mouse secondary antibodies (Amersham Biosciences, Piscataway, NJ) were used for detection. Chemiluminiscent substrates Super Signal West Pico and Femto (Pierce) were used for development. Images were obtained (Kodak Image Station 4000 R, Kodak, Rochester, NY) and digitized (UN-SCAN-IT, Silk Scientific, Inc, Orem, Utah) to compare labeling intensity. The net intensity of the signal detected for each immunoreactive band was normalized by using the net intensity of GAPDH immunoreactivity in each lane as a loading control. The normalized intensity of vehicle-treated cell lysates was used as a benchmark for comparison in each condition.

F-actin/total actin ratio: The relative amount of filamentous actin (F-actin) and globular actin (G-actin) in MDCK and PVD9902 cell lysates was measured using a commercially available kit (BK037, Cytoskeleton, Denver, CO). Cells were homogenized in a lysis buffer that stabilizes F-actin (50 mM PIPES, pH 6.9, 50 mM KCl, 5 mM $MgCl_2$, 5 mM EGTA, 5% glycerol,

0.1% Nonidet P40, 0.1% Triton X-100, 0.1% Tween 20, 0.1% 2-mercapto-ethanol, 0.001% Antifoam C, 1 mM ATP, 1 µg/ml pepstatin, 1 µg/ml leupeptin, 10 µg/ml benzamidine, 500 µg/ml tosyl arginine methyl ester). Cell lysates were centrifuged at 2000 rpm for 5 min to pellet unbroken cells, which were discarded. F-actin was separated from G-actin in the supernatant by centrifugation at 100,000g for 60 min at 37ºC. The F-actin-containing pellet was resuspended in ice cold water containing 2 µM cytochalasin D to the same volume as the G-actin-containing supernatant and incubated on ice for 1 hr to dissociate F-actin. Equal volumes of supernatant (containing G-actin) and dissociated pellet (F-actin) were subjected to immunoblot analysis using anti-actin antibody (AAN01; Cytoskeleton) and the F-actin/total actin ratio was determined by scanning densitometry as described.

Data analysis: All numerical results are reported as mean ± SEM. All graphs and regression fits were completed using Sigmaplot 2000 (v 6.0, SPSS Inc, Richmond, CA) and/or Excel (v 11.8, Microsoft Corp, Redmond, WA). The student's t-test (Sigmaplot) and ANOVA (Excel) were used for statistical analysis where appropriate. Differences between means were considered statistically significant if the probability of a type I error was <0.05. The time course for NC-1059 induced changes in g_{te} was determined by fitting a sigmoidal function (Eqn. 1) to values of g_{te} that were calculated every one hundred seconds throughout each experiment using the time of NC-1059 exposure as the starting point (i.e., t=0).

$$g_{te} = g_{te\,\min} + \frac{\Delta g_{te\,\max}}{1 + e^{-\left[\frac{t - t_0}{b}\right]}} \qquad \textbf{Eqn. 1}$$

In Eqn. 1, $g_{te\ \min}$ is the baseline conductance and $\Delta g_{te\ \max}$ is the peak change in conductance reached during the recording for each NC-1059 concentration. b is inversely proportional to the slope at half $\Delta g_{te\ \max}$ and t_0 is the time taken to reach half $\Delta g_{te\ \max}$. The data used for the fit from each experiment were restricted to ~300 s after the peak g_{te} was reached.

Results

NC-1059 induces a concentration dependent change in g_{te}.

The average change in the g_{te} in response to 100 and 200 μM NC-1059 as a function of time is provided in Fig 3.1. The graph reveals that the conductance increased with peptide exposure from 0.56 ± 0.09 mS cm^{-2} to a maximal value in about 30 min and remained elevated throughout the experiment. A significant increase in g_{te} was observed with 100 μM (8.52 ± 1.17 mS cm^{-2}) and several fold greater response was observed with 200 μM (32.32 ± 1.18 mS cm^{-2}) NC-1059. The half-maximal response occurred more quickly as indicated by lag time (t_0) and slope (b) with exposure to 200 μM (t_0 = 14.6 ± 0.6 and b = 4.71 ± 0.51 min) as compared to 100 μM NC-1059 (t_0 = 23.4 ± 1.0 and b = 7.01 ± 0.97 min).

g_{te} is a composite measure of the transcellular and paracellular conductances. The substantial increase in g_{te} after exposure to NC-1059 is consistent with the introduction of ion channels in the apical membrane and suggests that a paracellular route is opened, as reported previously (Broughman et al., 2004). As previously reported, exposure of MDCK monolayers to 60 μM NC-1059 resulted in a 5 fold increase in permeation of 9.5 kDa dextran, whereas permeation of ≥77 kDa dextran was not enhanced by NC-1059 (Broughman et al., 2004). However, further experiments conducted with other epithelial cell types showed that 200 μM NC-1059 enhanced permeation of 40 and 70 kDa dextran (Somasekharan et al., 2008). Hence experiments were conducted to measure permeation of intermediate sizes of dextran across MDCK monolayers, in the presence of NC-1059.

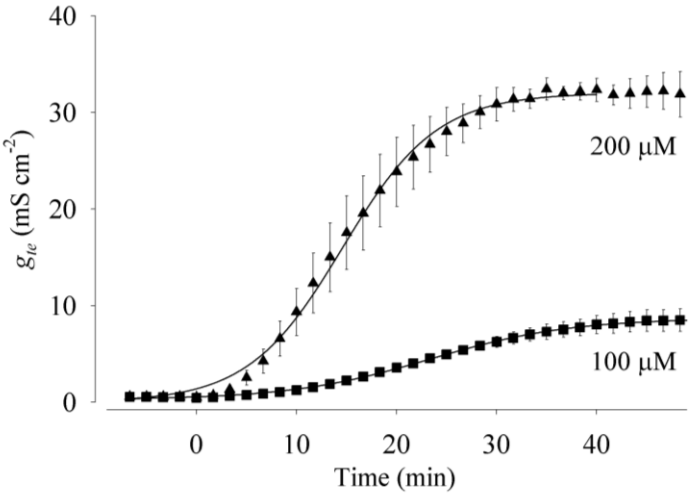

Figure 3.1 NC-1059 induces a concentration dependent change in g_{te}.

The average change in g_{te} (±SEM) with 100 μM (■) and 200 μM (▲) NC-1059 as a function of time is shown. Epithelial monolayers were exposed continuously to the indicated concentration of peptide in the apical bath beginning at the zero time point. The solid lines represent the best fit to Eqn. 1 to each data set. Parameters of the fit are reported in the text. Results are summarized from n=3.

NC-1059 can allow for the permeation of 40 and 70 kDa dextran across MDCK monolayers.

Dextran permeation across monolayers exposed to vehicle, 200 μM NC-1059 or EDTA in hypotonic buffer over a duration of 1 hr was measured (Fig 3.2). Monolayers exposed to EDTA showed a large enhancement in permeation for both 40 and 70 kDa dextran relative to vehicle treated monolayers. NC-1059 also enhanced permeation of 40 and 70 kDa dextran relative to vehicle treated monolayers. However the fold enhancement was small compared to EDTA, a compound that has a disruptive effect on epithelia. These results support observations made with other cell types (Martin et al., 2009; Somasekharan et al., 2008) and indicate that the paracellular route is partially opened by NC-1059 to allow permeation by various size dextrans across MDCK monolayers.

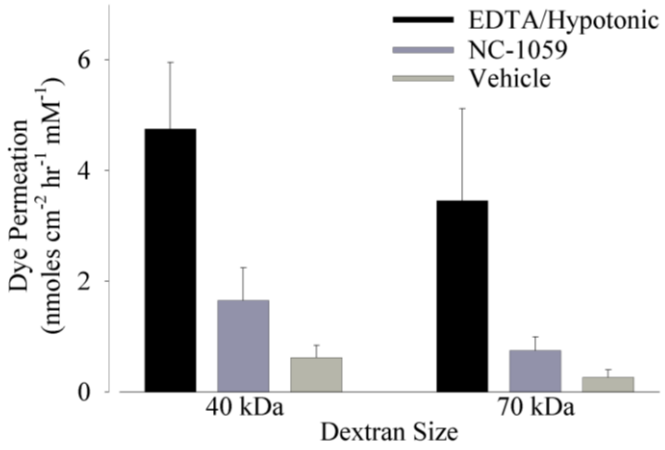

Figure 3.2 NC-1059 allows for the movement of uncharged molecules across MDCK epithelial monolayers.

FITC conjugated dextran of 40 and 70 kDa was added to the apical compartment and appearance of fluorescence in the basolateral compartment was quantified in the presence of one of three treatments (EDTA, NC-1059 or vehicle) as described in methods. Results are summarized from n=3.

Monolayers recover g_{te}.

The g_{te} of MDCK monolayers treated with 100 μM NC-1059 was observed to return to pretreatment levels within 48 hrs after exposure (Broughman et al., 2004). Hence experiments were conducted to compare the pattern of recovery in g_{te} in monolayers treated with 100 and 200 μM NC-1059.

The increase in g_{te} observed upon exposure to either 100 or 200 μM returned to pretreatment levels over a duration of 48 hrs (Fig 3.3). Monolayers were exposed to NC-1059 or vehicle for 60 min and then placed back in typical culture conditions for 24 or 48 hrs. Monolayers that were exposed to 100 (Fig 3.3A) or 200 μM NC-1059 (Fig 3.3B) for 60 min showed a significant increase in g_{te}. After 24 hrs the g_{te} decreased toward pretreatment levels and reached values that were less than 18% of the peak value with 100 μM and less than 12% of peak value with 200 μM, but remained significantly greater than pretreatment. In 48 hrs the g_{te} decreased further, to pretreatment levels.

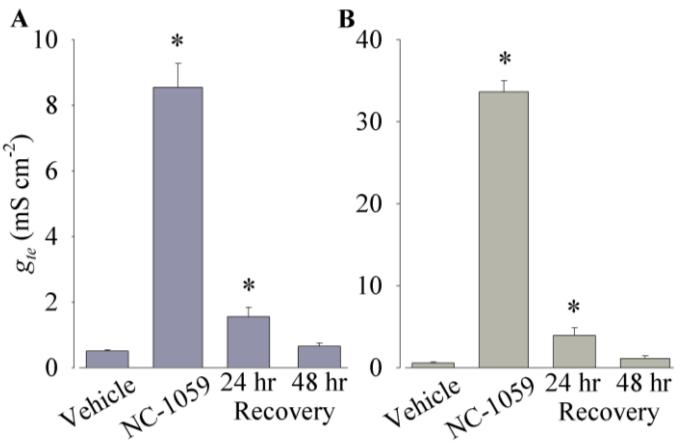

Figure 3.3 Monolayers exposed to 100 and 200 µM NC-1059 recover to pretreatment g_{te} within 48 hours.

Recovery in g_{te} after exposure to 100 µM (A) or 200 µM (B) NC-1059 is shown. Monolayers were exposed to vehicle or NC-1059 for 60 min and returned to the incubator. g_{te} was subsequently measured after 24 hrs and 48 hrs for each pair (vehicle and NC-1059 treated) of monolayers and results are summarized from n=3. Asterisk (*) indicates significant difference from vehicle.

NC-1059 has no apparent effect on epithelial cell density.

Media or buffer removed after cell monolayers were exposed to NC-1059 were indistinguishable from those that had been exposed to only the vehicle – there was no indication of cells or cell debris in the spent medium. Nonetheless, experiments were conducted to determine whether cell loss might account for the increase in conductance caused by NC-1059. g_{te} was assessed one or two days after seeding different densities of MDCK cells onto culture supports (Fig 3.4). Culturing $\leq 10^5$ cells for 24 or 48 hrs showed very high conductances of >40 mS cm^{-2} after 1 day or 2 days in culture. This outcome suggested that ≤100,000 cells is too few to form a confluent monolayer in the 1.13 cm^2 permeable supports within 2 days. When a high density of cells ($\geq 10^6$) was seeded, a low conductance of <1 mS cm^{-2} was observed within one day. It should be noted that MDCK cells typically grow to a density of ~10^6 cells cm^{-2}, or ~1.1×10^6 cells per Snapwell support. As shown in the figure, seeding 300,000 cells resulted in a conductance measured after 24 hrs that was greater than the conductance immediately following exposure to 100 µM NC-1059, and that, with an additional 24 hrs in culture conductance values approached those of a mature monolayer. These results suggest that >300,000 cells (i.e., a

virtually confluent monolayer) must be present on the permeable support following exposure to NC-1059 to achieve conductances of <5 mS cm^{-2} within 24 hours, as is observed. Normally ~2×10^5 cells were seeded onto permeable supports and cultured for 14 days prior to mounting in a modified Ussing chamber for assessing g_{te} and I_{sc} (e.g., Fig 3.3). If NC-1059 causes a loss of cells from the monolayer, more than 500,000 cells would have to have been lost to account for the highest conductance observed, an amount that would have been obvious when removing spent media. Furthermore, >300,000 cells would be required on the filter support to achieve the conductance that was measured after 24 hrs. The results suggest that cell loss from the monolayer and proliferation of remaining cells cannot account for the changes in conductance that are observed. Rather, the outcome suggests a change of tight junction permeability without a loss of epithelial cells from the confluent monolayer.

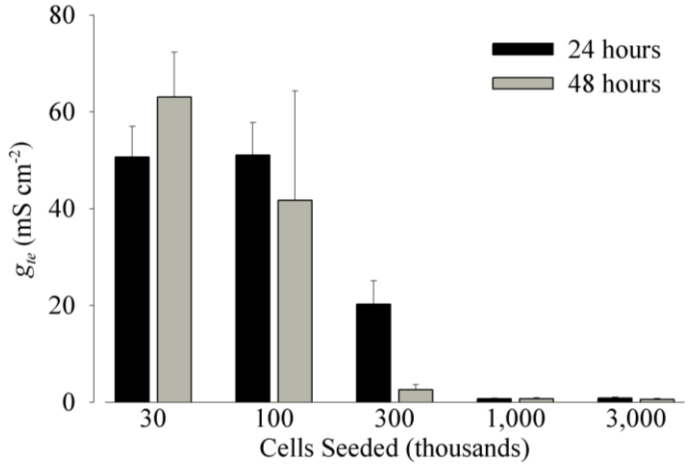

Figure 3.4 Low cell densities fail to form a resistive monolayer within 48 hours.

g_{te} was assessed in modified Ussing chambers 24 and 48 hrs following the seeding of the indicated number of cells on a permeable culture support (1.13 cm^2). Results are summarized from n=4-6 at each seeding density and time point.

NC-1059 has no effect on lactate dehydrogenase (LDH) release.

LDH release was measured to determine whether NC-1059 compromises cell membrane integrity and by inference, cell viability. A commercial kit was used in which florescence is proportional to LDH activity in the cell culture medium. In initial assays, MDCK cells were

cultured on 96-well plates to test for NC-1059 induced LDH release. MDCK cells exposed to NC-1059 (200 µM) for 60 min showed an LDH release that was not different from vehicle alone while paired cells exposed to EDTA (5 mM) exhibited significantly greater LDH release into the medium (Fig 3.5A). The effects of NC-1059 on LDH activity released from MDCK monolayers cultured on permeable supports was also tested. Similar with the result reported for cells grown on solid supports, the LDH activity released from NC-1059 treated cells was indistinguishable from those exposed to vehicle only, while EDTA exposure was associated with an apparent doubling of LDH activity in the apical medium (Fig 3.5B). These outcomes indicate that NC-1059 has no measurable effect on cell membrane integrity and thus, even at the concentration tested (200 µM) and the duration of exposure (60 min) there is no observable effect on cell viability.

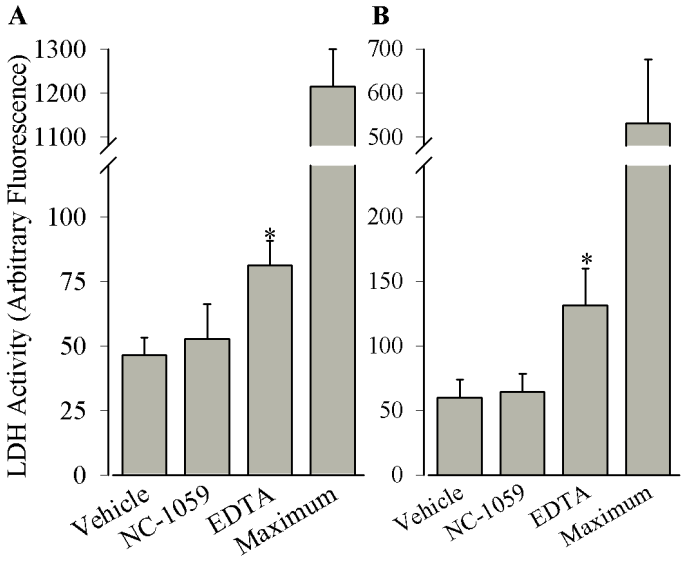

Figure 3.5 NC-1059 has no effect on cellular lactate dehydrogenase (LDH) release.

MDCK cells were grown on 96 well plates for three days (A) or on transwell permeable supports for 14 days (B) and exposed to NC-1059 (200 µM), EDTA (5 mM) or vehicle for 60 min. Cells in paired wells were lysed to determine maximum LDH activity. LDH activity in the apical medium is proportional to fluorescence at 590 nm. Results are summarized from 8 experiments on each cell culture platform. Asterisk (*) indicates significant difference from vehicle.

NC-1059 exposure causes actin reorganization.

Experiments were conducted to determine the effect of NC-1059 on actin organization as a function of time (Fig 3.6A). Images of the phalloidin (i.e., F-actin)-labeled monolayers were obtained as optical sections along the Z-axis. Sections were divided into apical, middle and basal regions and each panel presented in the figure is a composite projection of 4-6 optical sections. F-actin fibers are present throughout all portions of all cells in the monolayer. Each cell is circumscribed clearly by the perijunctional actomyosin ring in the apical region. There is also central punctate labeling of F-actin fibers in the apical region. The middle and basal sections show cortical actin filaments. In the most basal sections, actin filaments appear bundled and might constitute stress fibers. Exposure of the monolayer to NC-1059 (200 μM) for 5 min revealed little change in the F-actin labeling along the entire depth of the monolayer. The intensity of the labeling of central actin fibers and perijunctional actomyosin ring in some areas was reduced at 15 min. The images clearly show regions of the monolayer in which the apical sections exhibited no labeling while adjacent cells remained fully circumscribed. After 30 min of NC-1059 exposure an overall decrease in labeling intensity was observed in the apical, middle and basal sections of the Z-stack. Relative to the 15 minute time point, larger regions of the monolayer were devoid of F-actin labeling, especially at the apical regions. At the same time, the labeling of the perijunctional actomyosin ring was intensified in the remaining cells. After 60 min of NC-1059 exposure the labeling of apical actin fibers was dramatically reduced. There was a reduction in the punctate labeling of F-actin fibers apically and a pronounced decrease in labeling intensity of the perijunctional actomyosin ring. There was also a pronounced reduction in the labeling of fibers in the middle and basal portions of the cells. The reduction in the intensity of labeling both at the perijunctional actomyosin ring and F-actin fibers throughout the Z-stack suggested a disruption in the organization of the actin cytoskeleton in NC-1059 treated monolayers. Monolayers exposed to NC-1074, a scrambled sequence of NK_4-M2GlyR that does not elicit any changes in ion transport, showed a phalloidin labeling pattern comparable to vehicle exposed monolayers, which suggests that the effect on actin organization was specific to the NC-1059 sequence.

NC-1059 has a concentration dependent effect on g_{te} and it is likely that the effect of NC-1059 on actin organization might also follow a concentration dependent pattern. The patterns of actin organization in MDCK monolayers exposed to 100 and 200 μM NC-1059 reveal that there

is a modest but perceptible difference in the effect of these concentrations on actin organization (Fig 3.6B). Exposure of monolayers to 100 μM NC-1059 for 30 min caused a reduction in the labeling of the actin fibers along all regions of the Z-stack. Large areas showed a pronounced decrease in F-actin labeling intensity, both centrally and along the perijunctional actomyosin ring. However, some cells exhibited an enhanced intensity especially along the perijunctional actomyosin ring. After 60 min of exposure with 100 μM NC-1059, there was a decrease in labeling intensity of F-actin throughout most cells. The results observed with 200 μM NC-1059 were consistent with observations made in the previous experiment at the corresponding time points. The middle and basal sections show a further decrease in labeling intensity after 60 min of exposure with both concentrations. However it might be noted that after 60 min of exposure to 200 μM NC-1059, the labeling of the preijuntional actomyosin ring, although substantially decreased in intensity, is still circumscribing all cells.

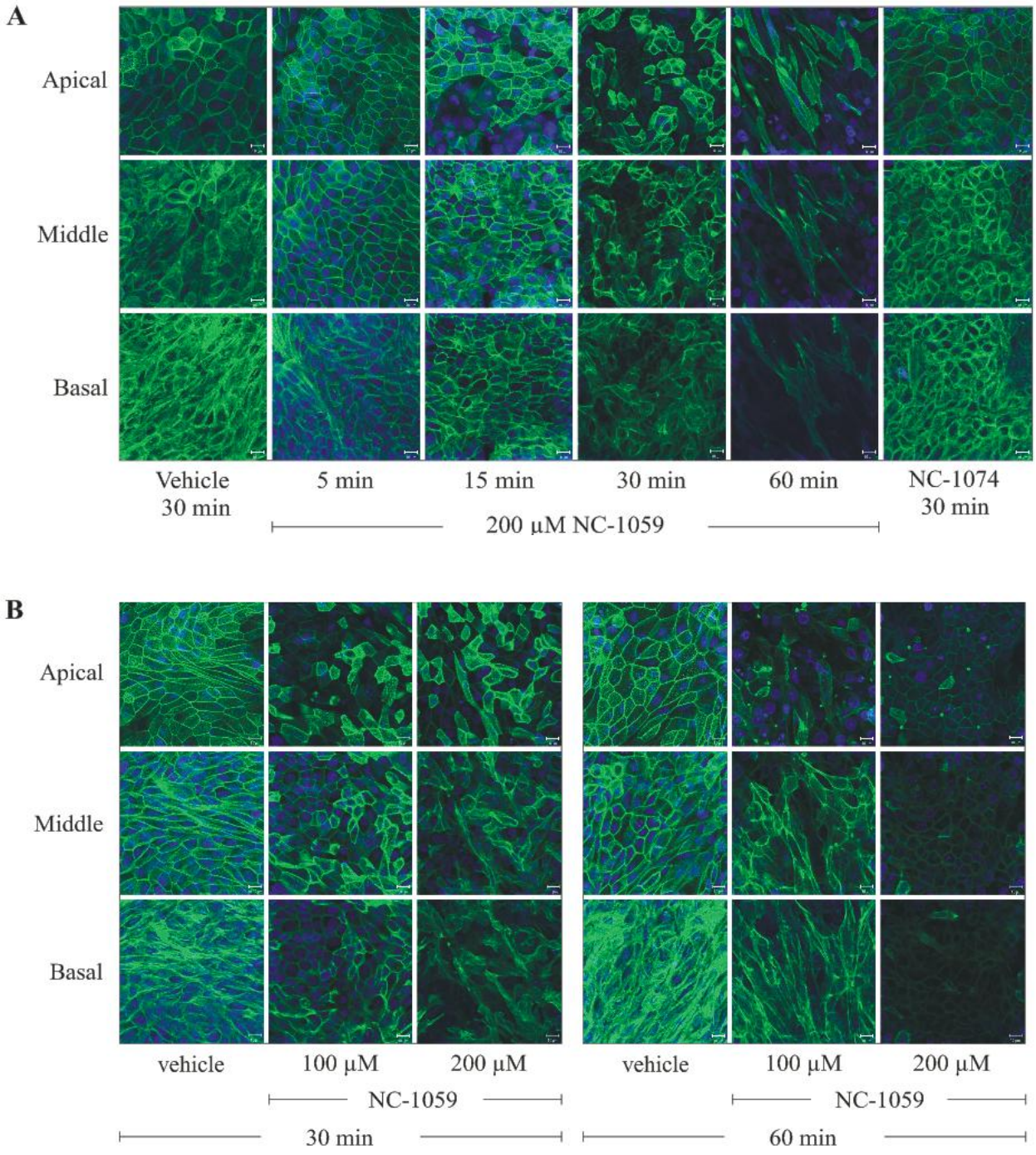

Figure 3.6 NC-1059 causes actin reorganization within MDCK cells.

A) Time course of the effects of NC-1059 on actin organization. Panels show images of monolayers labeled with Alexa-conjugated phalloidin. Images show typical F-actin labeling in monolayers that were exposed to vehicle, NC-1059 (200 µM), or NC-1074 (200 µM) for the indicated durations. B) Effect of 100 and 200 µM NC-1059 on actin organization. Monolayers were exposed to vehicle or NC-1059 at the

concentrations and durations indicated, and labeled with Alexa-conjugated phalloidin. All images are 3-D projections of the respective Z-stacks obtained using confocal microscopy. In both panels, the results are a typical example of n=4 and from paired monolayers.

NC-1059 alters the F-actin:total actin ratio in epithelial cell.

Immunoblotting was conducted to determine whether the abundance of F-actin is affected by NC-1059 exposure. Fig 3.7A includes immunoblots of G-actin (G) and F-actin (F) immunoreactivity derived from MDCK monolayers after apical exposure to vehicle, NC-1059 (200 μM) for 60 minutes, or NC-1059 for 60 minutes followed by 48 hrs recovery. Results from initial experiments showed little F-actin immunoreactivity in MDCK cells and densitometric analysis after background subtraction detected very low amounts (~10% of total actin), although the detection was consistent. Therefore, assays were conducted with 3T3 cells, which have been used for this assay by the manufacturer. Densitometric analysis revealed an F-actin:total actin (F:T) ratio of ~0.3, which is in the anticipated range. It was then speculated that epithelial cells may have a lower amount of actin or a lower F:T actin ratio and other epithelial cell lines were assessed. PVD9902 cells, which were derived from pig vas deferens and which exhibited an increase in transcellular conductance and paracellular permeation after apical NC-1059 exposure (Somasekharan et al., 2008) exhibited the highest F:T actin ratio of three epithelial cell types tested (Fig. 7; T84 cells revealed the lowest F:T actin ratio in basal conditions, ~5%, and were not used further). In basal conditions, the F:T actin ratio for PVD9902 cells was 16% and following exposure to NC-1059, the F:T actin ratio was reduced to 8%. After 48 hrs (the only time-point tested), the F:T actin ratio was indistinguishable from vehicle-treated monolayers. The results with PVD9902 cells are consistent with the outcomes shown in Fig. 6 for MDCK cells insofar as the amount of F-actin detectable after 60 min exposure to NC-1059 is extremely low and clearly reduced from pretreatment levels. The results with PVD9902 cells and T84 cells support the validity of the initial observations with MDCK cells showing very low F:T actin ratios in basal conditions. The ratio was reduced from 9.2±1.8% to 2.9±0.7% by NC-1059 exposure (Fig. 7). Like PVD9902 cells, the F:T actin ratio in MDCK cells returned to pretreatment levels within 48 hrs. Taken together, the results presented in Figs 3.6 and 3.7 show that NC-1059 causes rapid and substantial changes in the actin cytoskeleton. These changes are

observable in the same time-frame as changes in R_{te} and may be associated with changes in tight junction architecture.

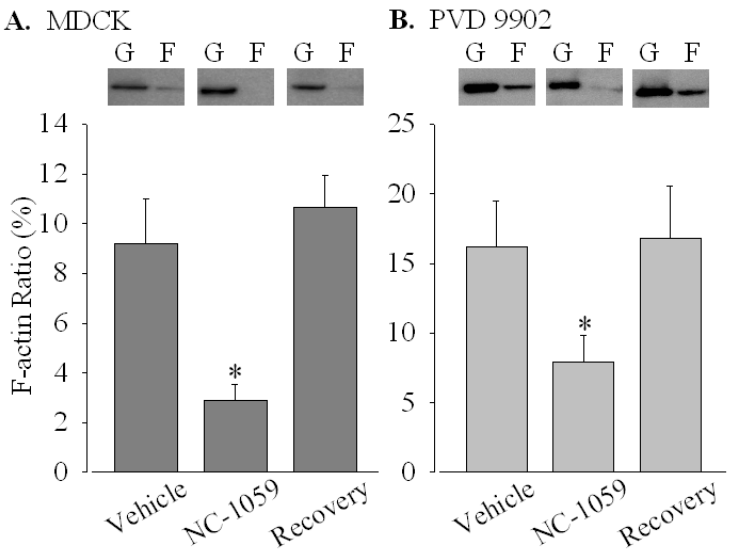

Figure 3.7 NC-1059 decreases the F-actin ratio in both MDCK cells (A) and PVD9902 cells (B).

Monolayers were exposed apically to vehicle or NC-1059 (200 μM) for 60 min and lysed immediately or the apical medium was refreshed and the cells were allowed to recover for 24 hr prior to cell lysis and analysis. Immunoreactivity of G-actin (G) and F-actin (F) was determined by densitometry as described in the text. Data are presented as F-actin to total actin ratio expressed as a percent. Results are summarized from n=4 for each cell type. Asterisk (*) indicates significant difference from vehicle.

NC-1059 alters the distribution of occludin and ZO-1.

NC-1059 exposure was associated with diminished immunoreactivity for the junctional proteins ZO-1 and occludin, with a more pronounced effect on ZO-1 (Fig 3.8A). Monolayers that were exposed to vehicle and labeled with anti-ZO-1 (red) and anti-occludin (green) antibodies showed strong immunoreactivity in the apical region of the MDCK monolayers. ZO-1 and occludin immunoreactivity localized at the tight junctions along cell-cell contact regions, as expected, and the epitopes appeared to colocalize, as shown in the merged image. Exposure of MDCK monolayers to NC-1059 (200 μM) for 5 min and 15 min showed apparent reductions in the intensity of labeling relative to vehicle treated monolayers. A pronounced reduction in ZO-1 immunoreactivity was observed within 30 min of exposure. After 30 min of exposure there was not only a reduction in intensity of ZO-1 labeling, but there appeared to be an absence of labeling

in several areas of the monolayer. Occludin immunoreactivity appeared to be slightly reduced in intensity, albeit to a less pronounced extent when compared to ZO-1. After 60 min of NC-1059 exposure, immunoreactivity to ZO-1 was negligible and the labeling for occludin appeared to be discontinuous with a pronounced reduction in intensity. Immunoreactivity to anti-occludin and anti-ZO-1 antibodies in monolayers that were exposed to NC-1074 for 30 min was comparable to vehicle.

The decrease in immunoreactivity of the junctional proteins followed a concentration dependent pattern in MDCK monolayers (Fig 3.8B). Monolayers that were vehicle treated for 30 or 60 min showed comparable patterns for both occludin and ZO-1 immunoreactivity. Exposure to 200 μM NC-1059 resulted in substantially diminished immunoreactivity for ZO-1 within 30 min. Monolayers exposed to 100 μM NC-1059 for 30 min showed immunolabeling for both ZO-1 and occludin comparable to a monolayer that was exposed only to vehicle for 30 min. After 60 min of exposure, both 100 and 200 μM NC-1059 showed a pronounced decrease in ZO-1 immunoreactivity and a discontinuous pattern of occludin immunoreactivity. The immunolabeled images suggested a concentration dependent effect on the localization or abundance of the junctional proteins occludin and ZO-1.

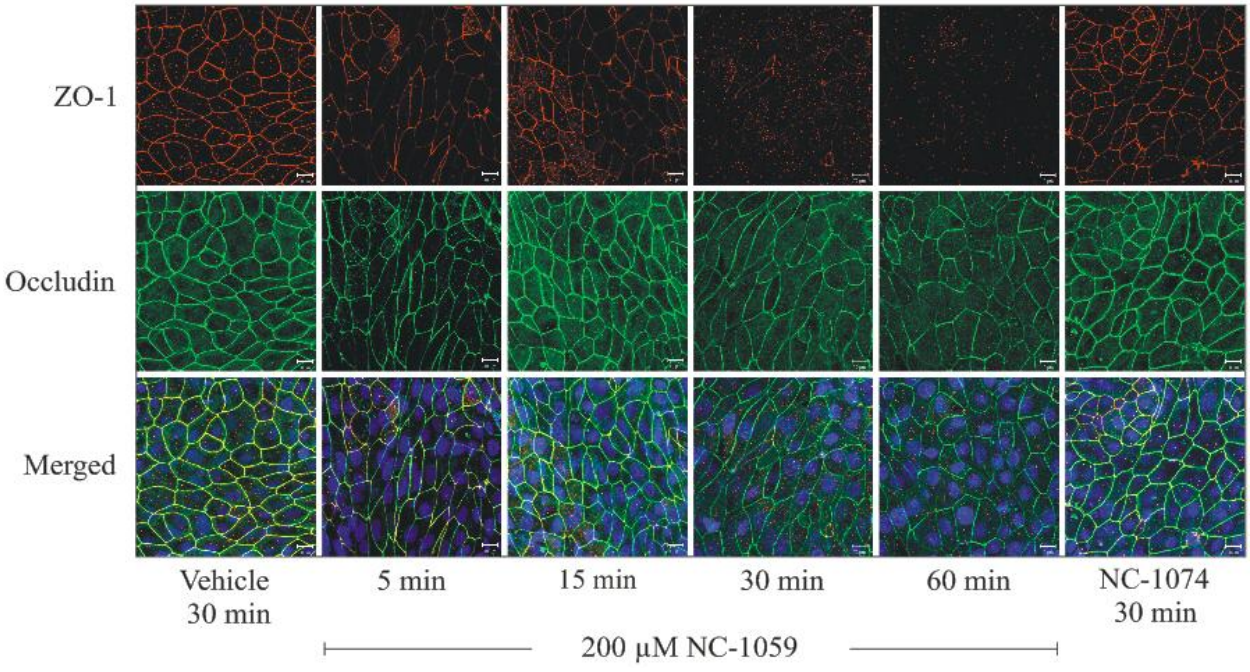

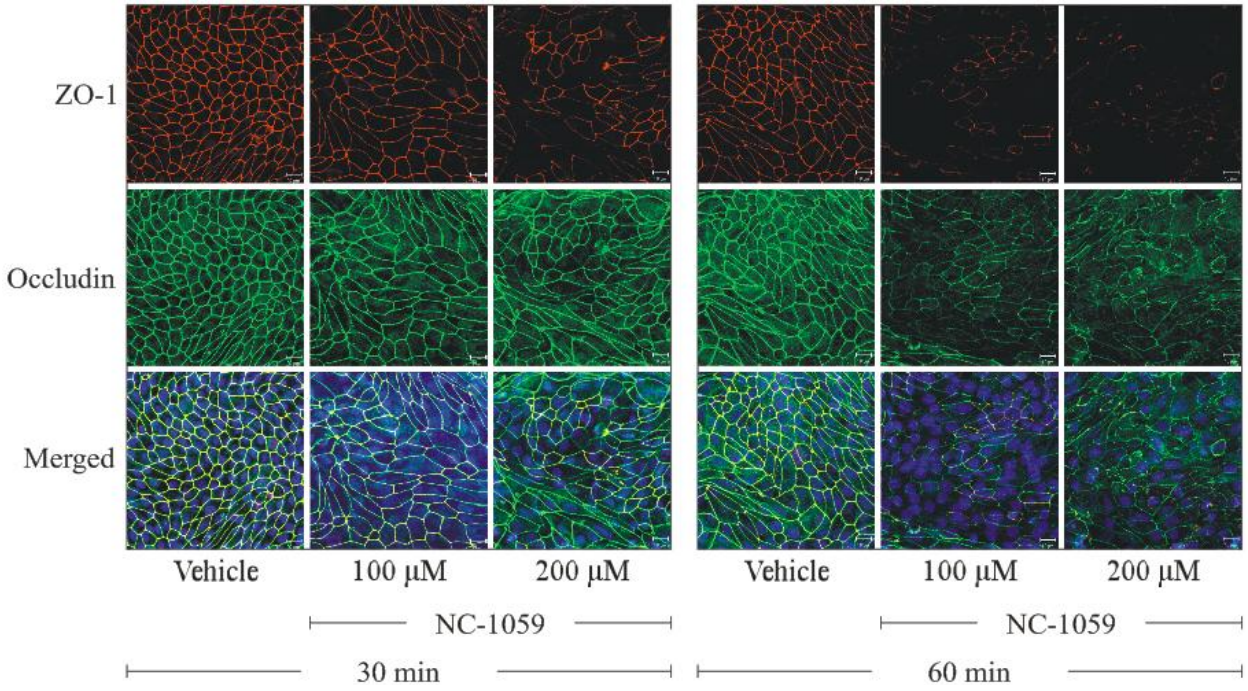

Figure 3.8 NC-1059 decreases ZO-1 and occludin immunoreactivity as a function of time and concentration.

A) Time course of the effects of NC-1059 on ZO-1 and occludin localization. Monolayers exposed to Ringer solution only for 30 min or to Ringer solution and 200 µM NC-1059 for 5, 15, 30 or 60 min were labeled with anti-ZO-1 (red, top panel) and anti-occludin antibodies (green, middle panel). NC-1074 is a peptide that has no effect on transepithelial resistance and is used as a negative control. The bottom panels show the merged image with labeling for the nucleus in blue. B) Concentration dependent effects of NC-1059 on ZO-1 and occludin localization. Monolayers were exposed to vehicle or exposed to 100 or 200 µM NC-1059 for 30 or 60 min and subsequently labeled with anti-ZO-1 and anti-occludin antibodies, as indicated. All images were obtained as Z-stacks using confocal microscopy. Images shown are the 3-D projection of the respective Z-stacks. Results are a typical representation of n=4 and results presented represent data from paired monolayers processed in parallel.

NC-1059 decreases the occludin and ZO-1 cellular abundance in a concentration dependent manner.

Immunoblotting was used to quantify the effect of 100 and 200 µM NC-1059 on the apparent abundance of occludin and ZO-1. Fig 3.9A is a typical immunoblot of protein extracted after apical exposure to 100 or 200 µM NC-1059 or vehicle for 30 or 60 min and labeled with

anti-ZO-1 antibodies. With 60 min exposure to NC-1059 there is an obvious decrease in labeling intensity. The average ZO-1 intensities normalized to GAPDH, which was used as a loading control, are presented in Fig 3.9B. The results suggested a concentration dependent decrease in ZO-1 immunoreactivity after 30 min that was reduced further and achieved statistical significance after 60 min of NC-1059 exposure. The intensities of vehicle exposed ZO-1 bands were comparable after 30 and 60 min.

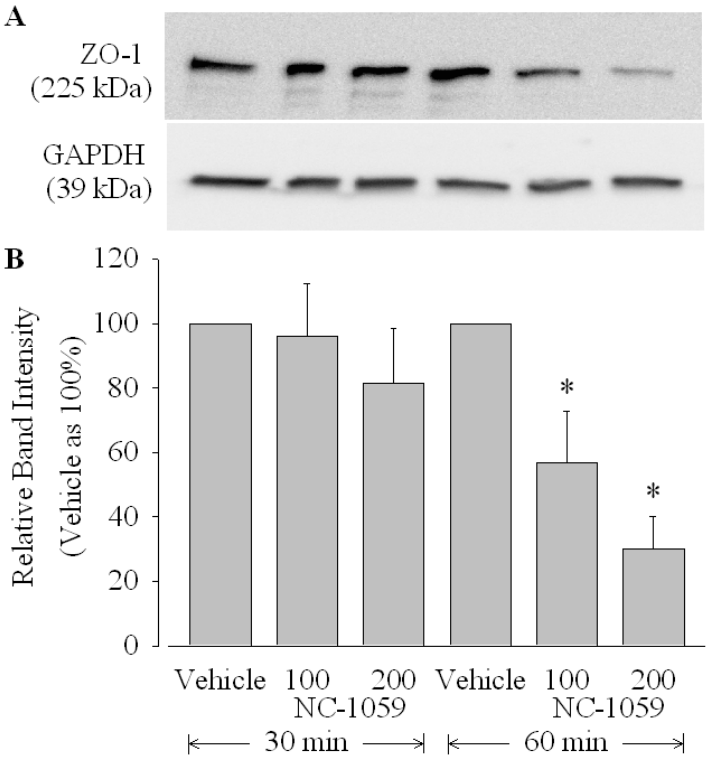

Figure 3.9 NC-1059 decreases cellular abundance of ZO-1 in a time and concentration dependent manner.

A) Typical blot showing ZO-1 immunoreactivity in monolayers that were exposed either to vehicle or NC-1059 at the indicated concentrations and durations. B) Average ZO-1 immunoreactivity determined by densitometry and normalized to intensity of the corresponding GAPDH immunoreactivity, then normalized to vehicle, which is treated as 100%. Results are summarized from n=5. Asterisk (*) indicates significant difference from vehicle.

Occludin immunoreactivity is also reduced by NC-1059 exposure. A typical immunoblot (Fig 3.10A) reveals a clear decrease in occludin immunoreactivity after 60 minutes of exposure to 100 and 200 μM NC-1059 relative to monolayers exposed to vehicle only for the same period

of time. The summarized results (Fig 3.10B) show decrease in the occludin immunoreactivity, after 30 min of exposure to 100 or 200 μM NC-1059, which is reduced further after 60 min. The results show both time- and concentration-dependent changes in cellular occludin abundance after exposure to NC-1059.

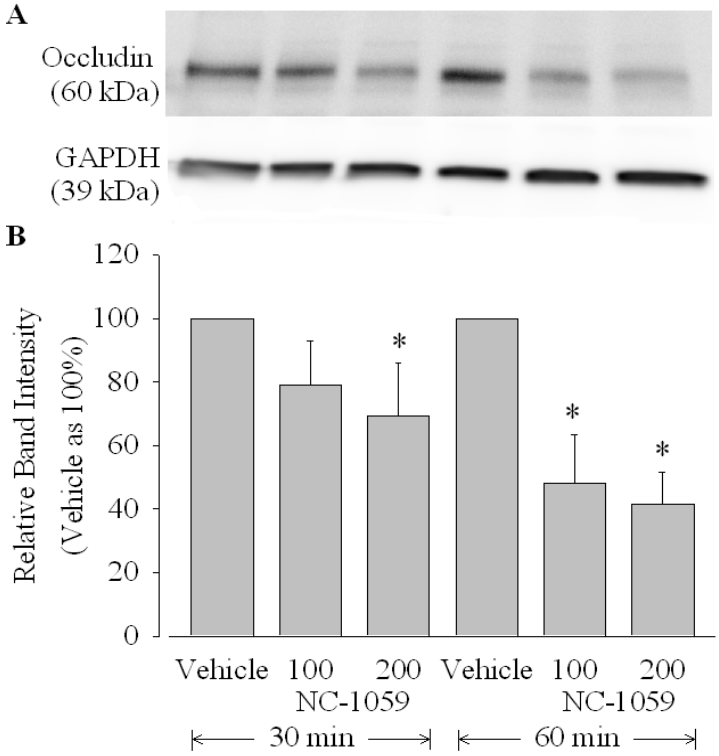

Figure 3.10 NC-1059 decreases cellular abundance of occludin in a time and concentration dependent manner.

A) Typical blot showing occludin immunoreactivity in monolayers that were exposed either to vehicle or NC-1059 at the indicated concentrations and durations. B) Average occludin immunoreactivity determined by densitometry and normalized to intensity of the corresponding GAPDH immunoreactivity, then normalized to vehicle, which is treated as 100%. Results are summarized from n=6. Asterisk (*) indicates significant difference from vehicle.

Monolayers recover localization of tight junction proteins.

Occludin and ZO-1 are localized at the tight junctions within 24 hr following exposure to NC-1059. The localization pattern after 48 hr is indistinguishable from vehicle treated monolayers (Fig 3.11). MDCK monolayers that were exposed to vehicle show that occludin and ZO-1 are localized as expected along the apical region of cell-cell contacts. MDCK monolayers

that were exposed to 200 μM NC-1059 for 1 hr exhibited little ZO-1 and occludin immunoreactivity along the expected apical cell-cell contacts contact points. NC-1059 treated monolayers that were recovered for 24 hrs showed anti-ZO-1 labeling at the tight junctions, similar to vehicle treated conditions. The intensity of occludin labeling was also recovered as compared to treatment with NC-1059 for 1 hr but appeared to be less pronounced as compared to the vehicle exposed monolayers. After 48 hr, ZO-1 immunolabeling showed a pattern and intensity comparable to control conditions, which suggests that localization of ZO-1 to the tight junctions was fully restored. Occludin localization along cell-cell contacts also appeared to be more pronounced after 48 hr of recovery.

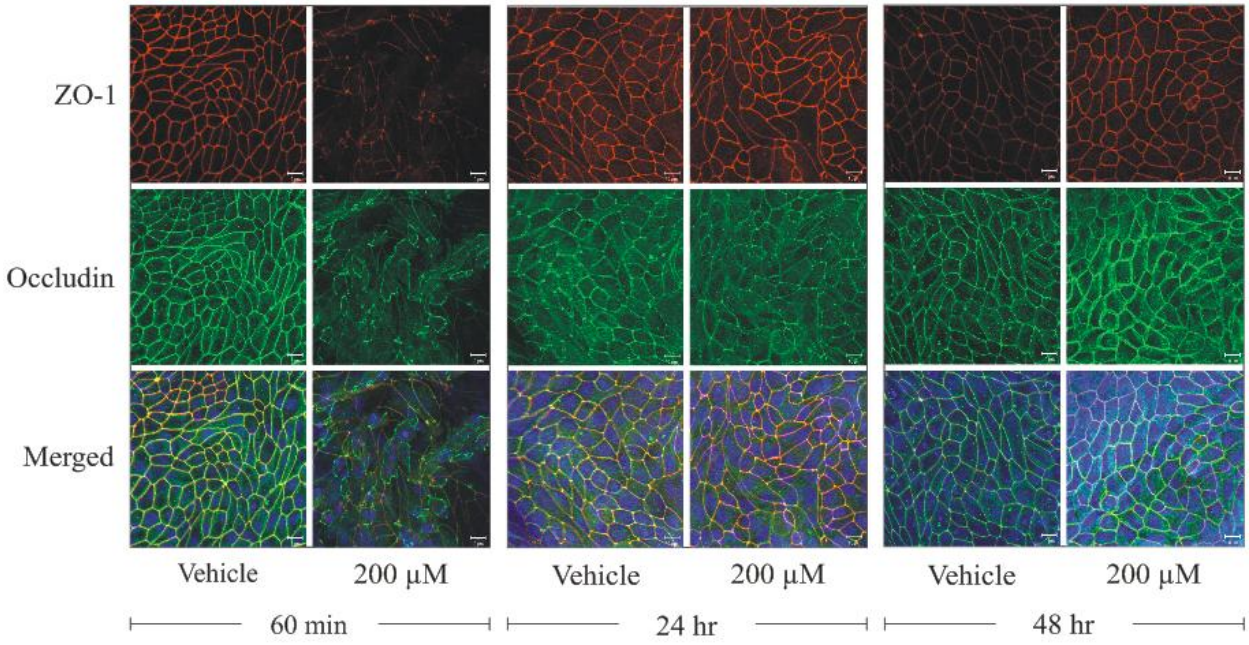

Figure 3.11 Occludin and ZO-1 immunoreactivities are again localized at all expected locations of tight junctions within 24 hrs following NC-1059 exposure.

MDCK monolayers were exposed apically to vehicle or NC-1059 (200 μM) for 1 hr after which the monolayers were either fixed or transferred to fresh culture medium and returned to the incubator for 24 or 48 hr before being fixed. Monolayers were then labeled with anti-occludin (green) and anti-ZO-1 (red) antibodies. Images were obtained as Z-stacks using confocal microscopy. Images shown are the 3-D projection of the respective Z-stacks. Results are a typical representation from n=2 for each condition.

NC-1059 alters the distribution and abundance of E-cadherin and β-catenin.

NC-1059 caused a decrease in immunoreactivity of the adheren junction proteins E-cadherin and β-catenin (Fig 3.12). Monolayers were exposed to 200 μM NC-1059 or vehicle for 30 or 60 minutes. Monolayers were subsequently fixed and labeled with anti-E-cadherin and anti-β-catenin antibodies. An orthogonal view showing the central optical slice (0.8 μM) and labeling along the x and y axis is presented for each condition. Monolayers that were vehicle treated for 30 or 60 minutes showed a reticular pattern of labeling along cell-cell contacts for E-cadherin and β-catenin, which is consistent with the localization of these proteins at the adheren junction. Exposure to 200 μM NC-1059 for 30 min resulted in decreased immunoreactivity of both E-cadherin and β-catenin and the labeling pattern appeared to be diffuse. After 60 minutes of exposure to 200 μM NC-1059, immunoreactivity of E-cadherin and β-catenin was diminished further.

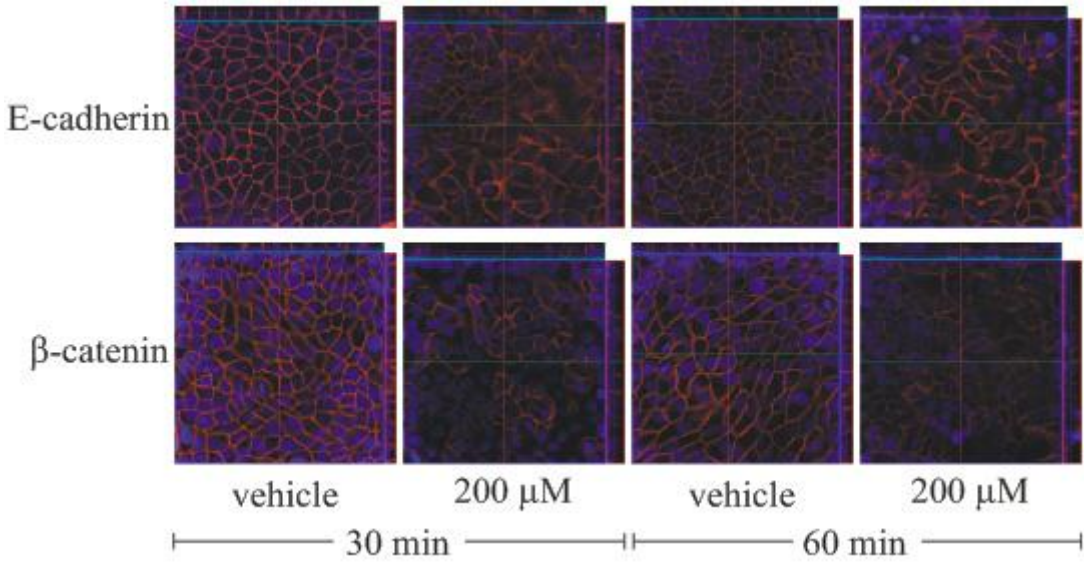

Figure 3.12 NC-1059 alters distribution of E-cadherin and β-catenin.

Monolayers were exposed to 200μM NC-1059 or vehicle (Ringer solution) for 30 or 60 minutes and labeled with anti-E-cadherin (red, top panel) and anti-β-catenin (red, bottom panel) antibodies. Images are presented as an orthogonal view showing a single optical slice (0.8μM) of the Z-stack and the labeling along x and y axis. Results are a typical representation from n=2 for each condition.

NC-1059 also reduced the cellular abundance of junctional proteins E-cadherin and β-catenin. Typical immunoblots of monolayers exposed to vehicle, 100 and 200 μM NC-1059 for

30 or 60 minutes and immunolabeled for E-cadherin and β-catenin, are represented in Figs 3.13 and 3.14, respectively.

Concentration-dependent reduction in intensity of the E-cadherin immunoreactivity after exposure to 100 and 200 μM NC-1059 is observed after 60 min (Fig 3.13), although only a trend is apparent after 30 minutes of NC-1059 exposure. A faint immunoreactive band is observed at ~80 kDa when monolayers are exposed to 200 μM NC-1059 for 60 min, which might represent a breakdown product of E-cadherin.

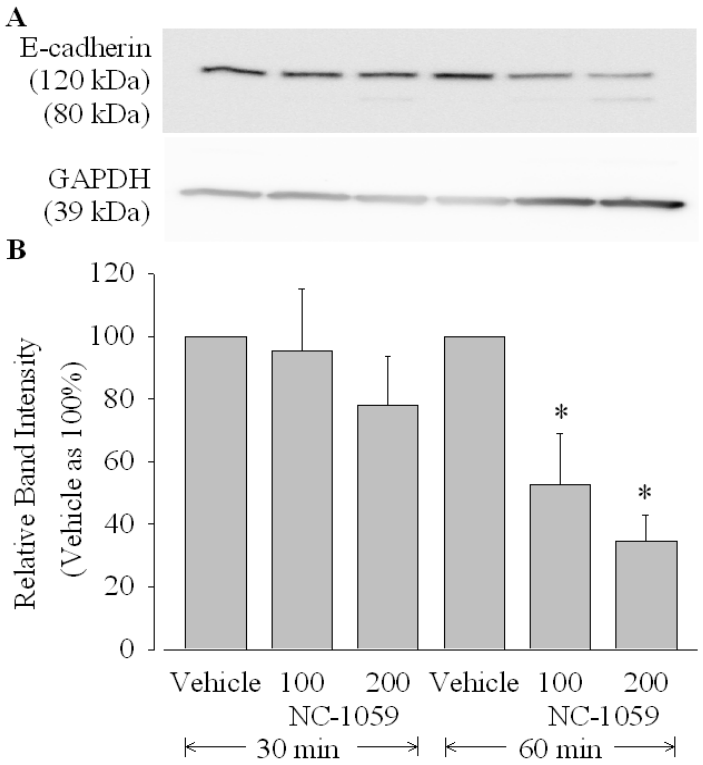

Figure 3.13 NC-1059 affects cellular abundance of E-cadherin in a time and concentration dependent manner.

A) Typical blot showing E-cadherin immunoreactivity in monolayers that were exposed either to vehicle or NC-1059 at the indicated concentrations and durations. B) Average E-cadherin immunoreactivity determined by densitometry and normalized to intensity of the corresponding GAPDH immunoreactivity, then normalized to vehicle, which is treated as 100%. Results are summarized from n=5. Asterisk (*) indicates significant difference from vehicle.

The effect of NC-1059 on cellular abundance of β-catenin (Fig 3.14) is modest compared with other junctional proteins. Although there is only modest decrease in β-catenin abundance

after exposure to 100 µM NC-1059 and 200 µM NC-1059 for 30 minutes, exposure to NC-1059 of 200 µM for 60 minutes resulted in a significantly decrease in immunoreactivity. The outcome suggests that NC-1059 affects adherens junction proteins as well as tight junction proteins in a concentration- and time- dependent trend.

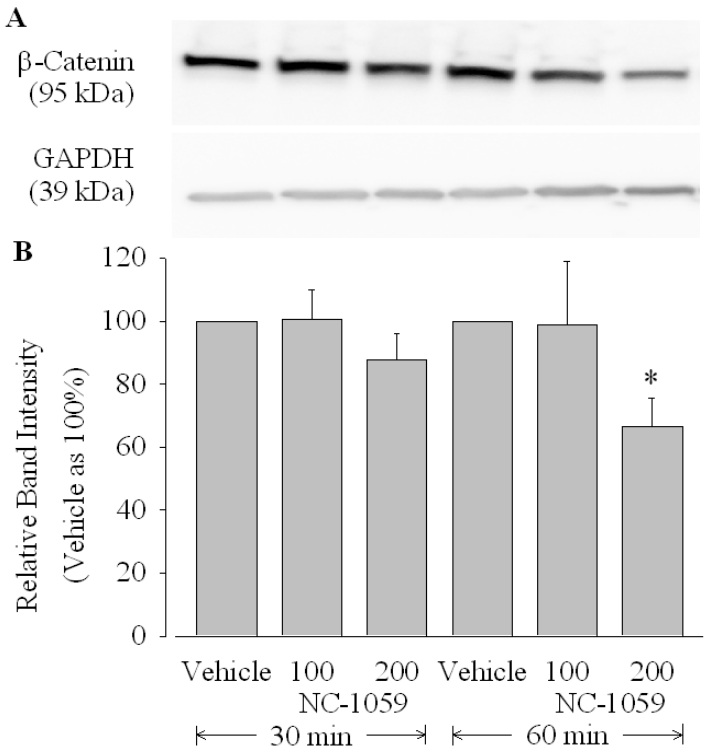

Figure 3.14 NC-1059 affects cellular abundance of β-catenin only at the highest concentration employed.

A) Typical blot showing β-catenin immunoreactivity in monolayers that were exposed either to vehicle or NC-1059 at the indicated concentrations and durations. B) Average β-catenin immunoreactivity determined by densitometry and normalized to intensity of the corresponding GAPDH immunoreactivity, then normalized to vehicle, which is treated as 100%. Results are summarized from n=5. Asterisk (*) indicates significant difference from vehicle.

Discussion

The results demonstrate that NC-1059 induces an increase in paracellular permeability that is associated with a change in organization of the actin cytoskeleton and a decrease in abundance of occludin and ZO-1 at the tight junctions. Proteins associated with the adherens junctions are similarly affected in that the organization and abundance of both E-cadherin and β-catenin are reduced. NC-1059 enhances g_{te} and solute permeability through a paracellular route in MDCK monolayers in a time- and concentration-dependent manner. The effects of NC-1059 on g_{te} and localization or abundance of the junctional proteins are transient insofar as the g_{te} and localization of tight junction proteins showed substantial recovery within 24 hr and complete recovery in 48 hr.

Apical exposure to NC-1059 caused a large increase in g_{te} in a concentration dependent manner. The rate of change in g_{te} and maximal g_{te} were significantly greater with 200 μM NC-1059 compared to 100 μM NC-1059. Previous studies showed that 60 μM NC-1059 enhanced permeability to dextran although no enhancement in the passage of dextrans as large as 77 kDa was observed (Broughman et al., 2004). Current results, however, show that 200 μM NC-1059, a concentration that is greater than previously tested, enhanced the permeation of both 40 and 70 kDa dextran several fold as compared to untreated monolayers. Permeation across epithelial barriers is the rate limiting step in the delivery of many drugs and since NC-1059 can enhance permeation of molecules as large as 70 kDa, it might provide the opportunity to be developed a co-therapeutic to enhance localized delivery of large molecular weight compounds that could be therapeutic if bioavailability issues can be overcome (e.g., interfering RNAs and antiviral drugs).

Apical exposure to 200 μM NC-1059 caused a reorganization of actin that was detectable as early as 15 min after exposure. There was a pronounced decrease in the intensity of labeling of F-actin by phalloidin after 30 min of NC-1059 exposure. Actin reorganization following exposure to both 100 and 200 μM NC-1059 exhibited a similar time course. F-actin is the polymerized form of actin and G-actin is the monomeric form. The polymerization is a reversible reaction and the two forms exist in equilibrium (Lodish et al., 1995). Loss of phalloidin labeling of F-actin filaments and decrease in F:T ratio suggests that there is an NC-1059 induced depolymerization of F-actin. This could be due to an increase in the rate of depolymerization or destabilization of the F-actin structure as is the case with compounds such as cytochalasin

(Lodish et al., 1995). Based on observations under physiological conditions, it was proposed that the contraction of the perijunctional actomyosin ring might play a role in enhancing permeability through the paracellular route (Lodish et al., 1995; Turner et al., 1997). Extracellular molecules such as cytochalasins (Madara, Barenberg & Carlson, 1986), protamines (Peixoto & Collares-Buzato, 2005) and ZOT (Fasano et al., 1995) are among several molecules that have been observed to enhance permeability by altering the organization of actin and specifically the perijunctional actomyosin ring. The NC-1059 induced increase in g_{te} is associated with actin rearrangement, which might be a common mechanism associated with increase in paracellular permeability.

NC-1059 treated MDCK monolayers show reduced immunoreactivity to antibodies against occludin and ZO-1, which suggests that NC-1059 causes a change in the distribution or abundance of these tight junction proteins. The distribution of ZO-1 appears to be altered to larger extent by 200 μM NC-1059 than by 100 μM at the 30 minute time point. Immunoblot analysis indicates NC-1059 decreases both occludin and ZO-1 abundance, which likely reflects enhanced breakdown of the junctional proteins, although the data do not rule out the possibility of an effect on synthesis. The loss of ZO-1, as indicated by immunoblotting also follows a concentration dependent trend. ZO-1 is a MAGUK protein that has several protein-protein interaction domains and hence serves as a scaffold for the interaction of junctional proteins and the actin cytoskeleton (Fanning et al., 1998; Funke, Dakoji & Bredt, 2005). ZO-1 interacts with occludin through its GUK domain and with actin through its C-terminus (Furuse et al., 1994; Li et al., 2005). Additionally occludin interacts with actin directly (Paris et al., 2008). Hence, the NC-1059 mediated change in actin organization might cause the loss of localization of occludin and ZO-1 at the tight junctions through its direct and indirect interactions with these proteins, ultimately leading to the disruption of barrier integrity.

NC-1059 also affects the distribution and cellular abundance of the adheren junction proteins, E-cadherin and, to a lesser extent, β-catenin. The immunoblot for E-cadherin shows the appearance of an immunoreactive band with greater mobility, perhaps suggesting that E-cadherin is cleaved by a specific protease. Breakdown of E-cadherin has been reported in the case of ATP depletion (Bush, Tsukamoto & Nigam, 2000) and also implicated in the effects on paracellular permeability by the zinc metalloprotease, *Bacteroides fragilis* toxin (Richard et al., 1999; Wu et al., 1998). The detection of an 80 kDa fragment is unusual since metalloproteases cause

ectodomain shedding with loss of the 80 kDa fragment and detection of only a 30-40 kDa fragment in other systems (Wu et al., 2007). Nevertheless the results are consistent with a protease activity. The intensity of β-catenin localized at the adherens junctions is also diminished, but the effect of NC-1059 on overall abundance is modest. Only at the highest concentration and longest duration of exposure was a significant effect observed. The relatively modest effect on abundance might reflect the multiple roles of β-catenin in the cell. β-catenin not only plays a central function in bridging cadherins to actins in adheren junctions, but also is a key mediator of the Wnt-signaling pathway. Thus the total amount of β-catenin is highly controlled and changes in the amount associated with adherens junctions maybe difficult to detect on the cytosolic background.

The effect of NC-1059 is transient. Despite the apparent reduction in F-actin, especially in the basal region of the cells, the monolayers remained adherent and g_{te} recovered to pretreatment levels within 48 hours, with greater than 85% of the recovery in the first 24 hours. Within 24 hrs there was obvious recovery of ZO-1 localization to the cell periphery in the monolayers and occludin also recovered, although to a lesser extent. Recovery could involve either synthesis of new protein or recruitment from a preexisting or recycling pool. The reduction in overall immunoreactivity in Western blots argues against recycling of protein. Moreover the recovery in g_{te} to pretreatment values requires more than 24 hours, which suggest that recovery might require synthesis and assembly of the junctional proteins. Localization of junctional proteins after 48 hrs is comparable to untreated monolayers. ZO-1 is proposed to be an early player in the assembly of junctional proteins (McNeil, Capaldo & Macara, 2006). Hence recovery in ZO-1 might be significant in the recovery of $g_{te.}$

The transient effect of NC-1059 on barrier function is particularly significant in developing a co-therapeutic to enhance delivery of drugs across epithelial barriers. ‘Absorption enhancers’ are being developed to deliver clinically relevant therapeutics across epithelial barriers. Molecules that are hydrophilic and/or large cannot easily permeate epithelial barriers. Systemic drug delivery requires larger doses of drugs and is therefore associated with potential side effects (Torchilin, 2000). Several barrier epithelia such as intestinal, airway and corneal/conjuctival epithelia are potential targets for localized drug delivery (Edward & Prausnitz, 2001; Ghandehari et al., 1997). Results presented in this paper show that NC-1059 enhances the permeation of molecules as large as 70 kDa across MDCK epithelial monolayers.

The effects on permeability can be generalized to several other epithelial cell lines derived from a variety of sources (Martin et al., 2009; Somasekharan et al., 2008).

In summary, NC-1059 is a channel-forming peptide that reversibly modulates epithelial conductance and enhances permeability through the paracellular pathway. This may be caused by the reversibly altered organization of actin and localization of junctional proteins. Additional studies are required to determine the signaling pathways that link NC-1059 exposure to transient changes in the paracellular pathway.

Acknowledgements:

The authors extend sincere thanks to Dr. Rebecca Quesnell and Dr. Yasuaki Hiromasa for technical assistance. This article is contribution #08-209-J from the Kansas Agriculture Station.

This study was supported by the NIH (GM 074096 to JMT) and used the confocal microscopy core facility provided by the COBRE Epithelial Function in Health and Disease (P20 RRO17686).

References

Broughman, J.R., Brandt, R.M., Hastings, C., Iwamoto, T., Tomich, J.M., Schultz, B.D. 2004. Channel-forming peptide modulates transepithelial electrical conductance and solute permeability. *Am J Physiol Cell Physiol* **286:**C1312-23

Broughman, J.R., Mitchell, K.E., Sedlacek, R.L., Iwamoto, T., Tomich, J.M., Schultz, B.D. 2001. NH(2)-terminal modification of a channel-forming peptide increases capacity for epithelial anion secretion. *Am J Physiol Cell Physiol* **280:**C451-8

Broughman, J.R., Shank, L.P., Prakash, O., Schultz, B.D., Iwamoto, T., Tomich, J.M., Mitchell, K. 2002. Structural implications of placing cationic residues at either the NH2- or COOH-terminus in a pore-forming synthetic peptide. *J Membr Biol* **190:**93-103

Bush, K.T., Tsukamoto, T., Nigam, S.K. 2000. Selective degradation of E-cadherin and dissolution of E-cadherin-catenin complexes in epithelial ischemia. *Am J Physiol Renal Physiol* **278:**F847-52

Carlin, R.W., Sedlacek, R.L., Quesnell, R.R., Pierucci-Alves, F., Grieger, D.M., Schultz, B.D. 2006. PVD9902, a porcine vas deferens epithelial cell line that exhibits neurotransmitter-stimulated anion secretion and expresses numerous HCO3(-) transporters. *Am J Physiol Cell Physiol* **290:**C1560-71

Chung, N.P., Mruk, D., Mo, M.Y., Lee, W.M., Cheng, C.Y. 2001. A 22-amino acid synthetic peptide corresponding to the second extracellular loop of rat occludin perturbs the blood-testis barrier and disrupts spermatogenesis reversibly in vivo. *Biol Reprod* **65:**1340-51

Edward, A., Prausnitz, M.R. 2001. Predicted permeability of the cornea to topical drugs. *Pharm Res* **18:**1497-508

Fanning, A.S., Jameson, B.J., Jesaitis, L.A., Anderson, J.M. 1998. The tight junction protein ZO-1 establishes a link between the transmembrane protein occludin and the actin cytoskeleton. *J Biol Chem* **273:**29745-53

Fasano, A., Fiorentini, C., Donelli, G., Uzzau, S., Kaper, J.B., Margaretten, K., Ding, X., Guandalini, S., Comstock, L., Goldblum, S.E. 1995. Zonula occludens toxin modulates tight junctions through protein kinase C-dependent actin reorganization, in vitro. *J Clin Invest* **96:**710-20

Fasano, A., Uzzau, S., Fiore, C., Margaretten, K. 1997. The enterotoxic effect of zonula occludens toxin on rabbit small intestine involves the paracellular pathway. *Gastroenterology* **112:**839-46

Funke, L., Dakoji, S., Bredt, D.S. 2005. Membrane-associated guanylate kinases regulate adhesion and plasticity at cell junctions. *Annu Rev Biochem* **74:**219-45

Furuse, M., Itoh, M., Hirase, T., Nagafuchi, A., Yonemura, S., Tsukita, S. 1994. Direct association of occludin with ZO-1 and its possible involvement in the localization of occludin at tight junctions. *J Cell Biol* **127:**1617-26

Ghandehari, H., Smith, P.L., Ellens, H., Yeh, P.Y., Kopecek, J. 1997. Size-dependent permeability of hydrophilic probes across rabbit colonic epithelium. *J Pharmacol Exp Ther* **280:**747-53

Gumbiner, B.M. 2005. Regulation of cadherin-mediated adhesion in morphogenesis. *Nat Rev Mol Cell Biol* **6:**622-34

Hartsock, A., Nelson, W.J. 2008. Adherens and tight junctions: Structure, function and connections to the actin cytoskeleton. *Biochim Biophys Acta* **1778:**660-9

Li, Y., Fanning, A.S., Anderson, J.M., Lavie, A. 2005. Structure of the conserved cytoplasmic C-terminal domain of occludin: identification of the ZO-1 binding surface. *J Mol Biol* **352:**151-64

Lodish, H., Baltimore, D., Berk, A., Zipursky, L., Matsudara, P., Darnell, J. 1995. Molecular Cell Biology. W.H.Freeman and Company, New York

Madara, J.L. 1998. Regulation of the movement of solutes across tight junctions. *Annu Rev Physiol* **60:**143-59

Madara, J.L., Barenberg, D., Carlson, S. 1986. Effects of cytochalasin D on occluding junctions of intestinal absorptive cells: further evidence that the cytoskeleton may influence paracellular permeability and junctional charge selectivity. *J Cell Biol* **102:**2125-36

Martin, J., Malreddy, P., Iwamoto, T., Freeman, L.C., Davidson, H.J., Tomich, J.M., Schultz, B.D. 2009. NC-1059, a channel-forming peptide modulates drug delivery across in vitro corneal epithelium. *Invest Ophthalmol Vis Sci*

McLaughlin, J., Padfield, P.J., Burt, J.P., O'Neill, C.A. 2004. Ochratoxin A increases permeability through tight junctions by removal of specific claudin isoforms. *Am J Physiol Cell Physiol* **287:**C1412-7

McNeil, E., Capaldo, C.T., Macara, I.G. 2006. Zonula occludens-1 function in the assembly of tight junctions in Madin-Darby canine kidney epithelial cells. *Mol Biol Cell* **17:**1922-32

Moore, R., Pothoulakis, C., LaMont, J.T., Carlson, S., Madara, J.L. 1990. C. difficile toxin A increases intestinal permeability and induces Cl- secretion. *Am J Physiol* **259:**G165-72

Nava, P., Lopez, S., Arias, C.F., Islas, S., Gonzalez-Mariscal, L. 2004. The rotavirus surface protein VP8 modulates the gate and fence function of tight junctions in epithelial cells. *J Cell Sci* **117:**5509-19

Paris, L., Tonutti, L., Vannini, C., Bazzoni, G. 2008. Structural organization of the tight junctions. *Biochim Biophys Acta* **1778:**646-59

Peixoto, E.B., Collares-Buzato, C.B. 2005. Protamine-induced epithelial barrier disruption involves rearrangement of cytoskeleton and decreased tight junction-associated protein expression in cultured MDCK strains. *Cell Struct Funct* **29:**165-78

Rajasekaran, A.K., Hojo, M., Huima, T., Rodriguez-Boulan, E. 1996. Catenins and zonula occludens-1 form a complex during early stages in the assembly of tight junctions. *J Cell Biol* **132:**451-63

Richard, J.F., Petit, L., Gibert, M., Marvaud, J.C., Bouchaud, C., Popoff, M.R. 1999. Bacterial toxins modifying the actin cytoskeleton. *Int Microbiol* **2:**185-94

Schipper, N.G., Varum, K.M., Artursson, P. 1996. Chitosans as absorption enhancers for poorly absorbable drugs. 1: Influence of molecular weight and degree of acetylation on drug transport across human intestinal epithelial (Caco-2) cells. *Pharm Res* **13:**1686-92

Schneeberger, E.E., Lynch, R.D. 2004. The tight junction: a multifunctional complex. *Am J Physiol Cell Physiol* **286:**C1213-28

Somasekharan, S., Brandt, R., Iwamoto, T., Tomich, J.M., Schultz, B.D. 2008. Epithelial barrier modulation by a channel forming peptide. *J Memb Biol* **222:**17-30

Tavelin, S., Hashimoto, K., Malkinson, J., Lazorova, L., Toth, I., Artursson, P. 2003. A new principle for tight junction modulation based on occludin peptides. *Mol Pharmacol* **64:**1530-40

Tomich, J.M., Wallace, D., Henderson, K., Mitchell, K.E., Radke, G., Brandt, R., Ambler, C.A., Scott, A.J., Grantham, J., Sullivan, L., Iwamoto, T. 1998. Aqueous solubilization of

transmembrane peptide sequences with retention of membrane insertion and function. *Biophys J* **74:**256-67

Torchilin, V.P. 2000. Drug targeting. *Eur J Pharm Sci* **11 Suppl 2:**S81-91

Turner, J.R., Rill, B.K., Carlson, S.L., Carnes, D., Kerner, R., Mrsny, R.J., Madara, J.L. 1997. Physiological regulation of epithelial tight junctions is associated with myosin light-chain phosphorylation. *Am J Physiol* **273:**C1378-85

Wallace, D.P., Tomich, J.M., Iwamoto, T., Henderson, K., Grantham, J.J., Sullivan, L.P. 1997. A synthetic peptide derived from glycine-gated Cl- channel induces transepithelial Cl- and fluid secretion. *American Journal of Physiology* **272:**C1672-9

Wong, V., Gumbiner, B.M. 1997. A synthetic peptide corresponding to the extracellular domain of occludin perturbs the tight junction permeability barrier. *J Cell Biol* **136:**399-409

Wu, S., Lim, K.C., Huang, J., Saidi, R.F., Sears, C.L. 1998. Bacteroides fragilis enterotoxin cleaves the zonula adherens protein, E-cadherin. *Proc Natl Acad Sci U S A* **95:**14979-84

Wu, S., Rhee, K.J., Zhang, M., Franco, A., Sears, C.L. 2007. Bacteroides fragilis toxin stimulates intestinal epithelial cell shedding and gamma-secretase-dependent E-cadherin cleavage. *J Cell Sci* **120:**1944-52

Wu, S., Shin, J., Zhang, G., Cohen, M., Franco, A., Sears, C.L. 2006. The Bacteroides fragilis toxin binds to a specific intestinal epithelial cell receptor. *Infect Immun* **74:**5382-90